TALK @ iit iCub ISTITUTO ITALIANO DI TECNOLOGIA iCUB FACILITY

Istituto Italiano di Tecnologia - IIT

Genova, January 23, 2019

Control schemes for safe human-robot interaction

Alessandro De Luca

Dipartimento di Ingegneria Informatica, Automatica e Gestionale (DIAG)

www.diag.uniroma1.it/deluca

SAPIENZA UNIVERSITÀ DI ROMA

Human-friendly robotics

The domain of physical and cognitive HRI

traditional robotics

replacing humans

human-friendly robotics

collaborating with humans

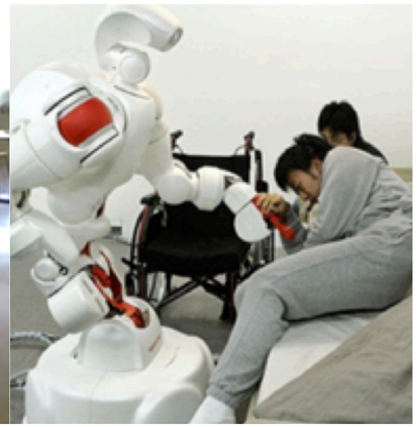

co-workers on factory floor

personal robots in service

Collision and contact handling

Basic safety-related control problems in pHRI

collision detection/isolation and reaction
(**without** the use of external sensing)

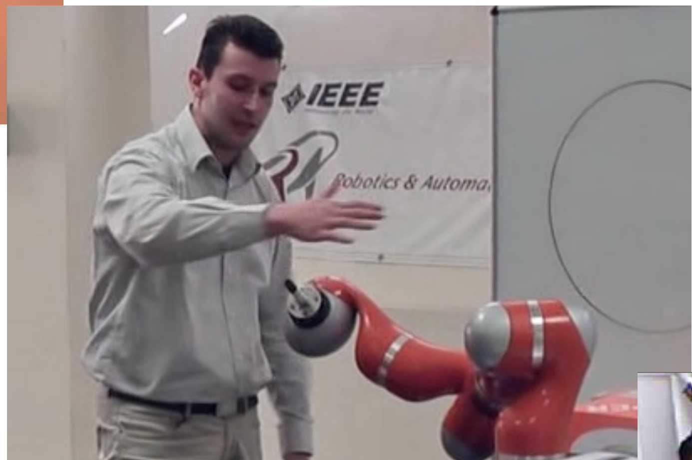

continuous
collision avoidance
(while the task is running)

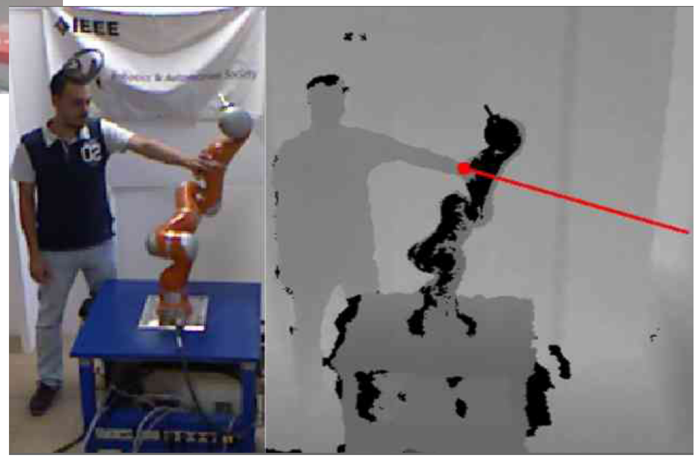

estimation and control
of intentional forces
exchanged at the contact
(**without** force or touch sensors)

Safety

Safety is the most important feature of a robot that has to work close to human beings

Classical solutions preserving safety in industrial environments – cages, stop/slow down robot motion in presence of humans **[ISO 10218, TS 15066]** – are not appropriate for collaborative pHRI

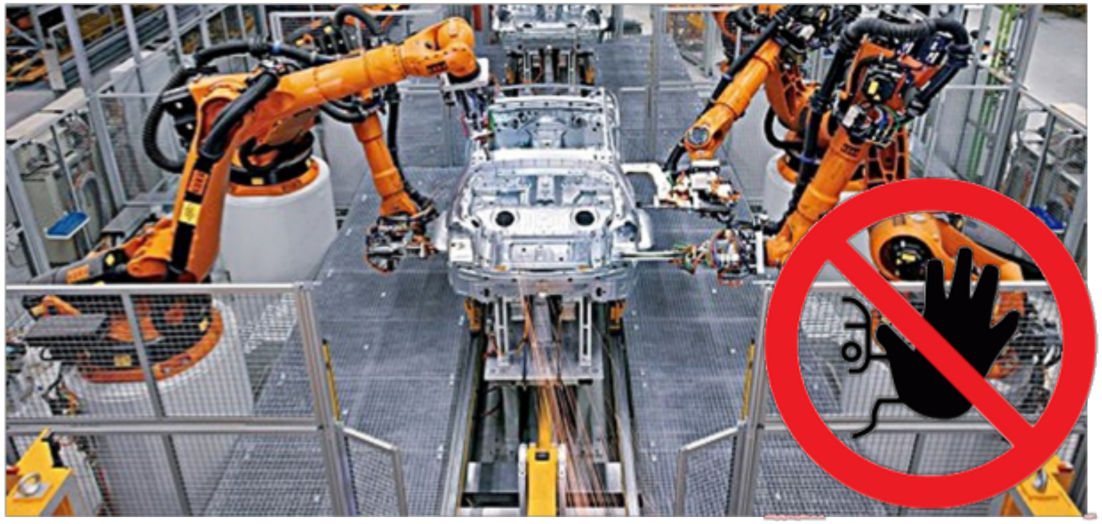

Physical HRI

Hierarchy of consistent behaviors

Safety

Coexistence

Coexistence is the robot capability of sharing the workspace with other entities, most relevant humans

Human (and robot!) safety requirements must be consistently guaranteed (i.e., **safe coexistence**)

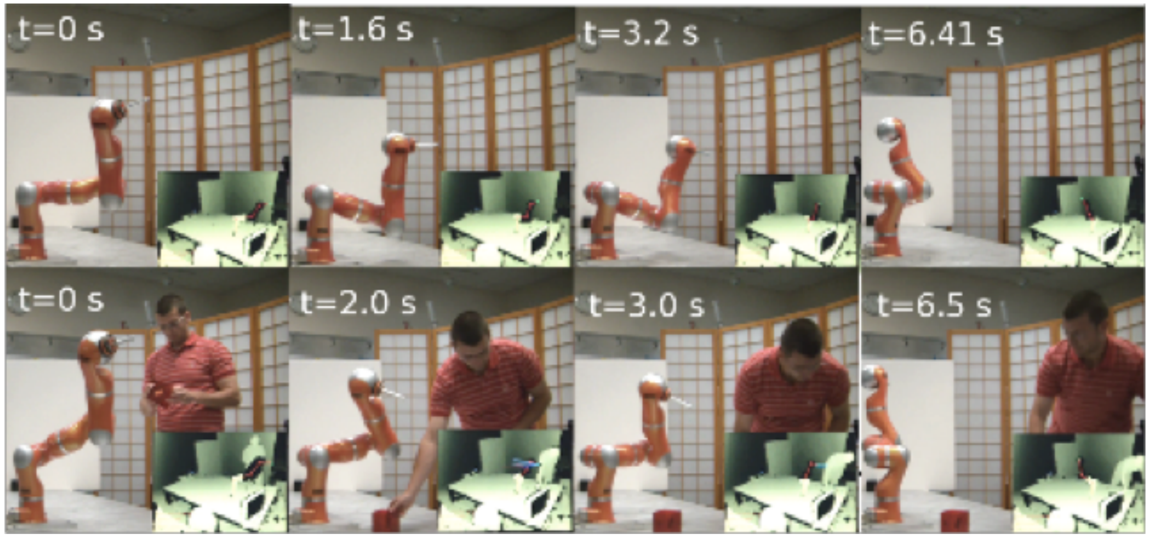

original robot task

safe HR coexistence

A control architecture for physical HRI

Hierarchy of consistent behaviors (BioRob 2012)

Collaboration occurs when the robot performs complex tasks with direct human interaction and coordination

Two modalities which are not mutually exclusive: contactless and **physical**

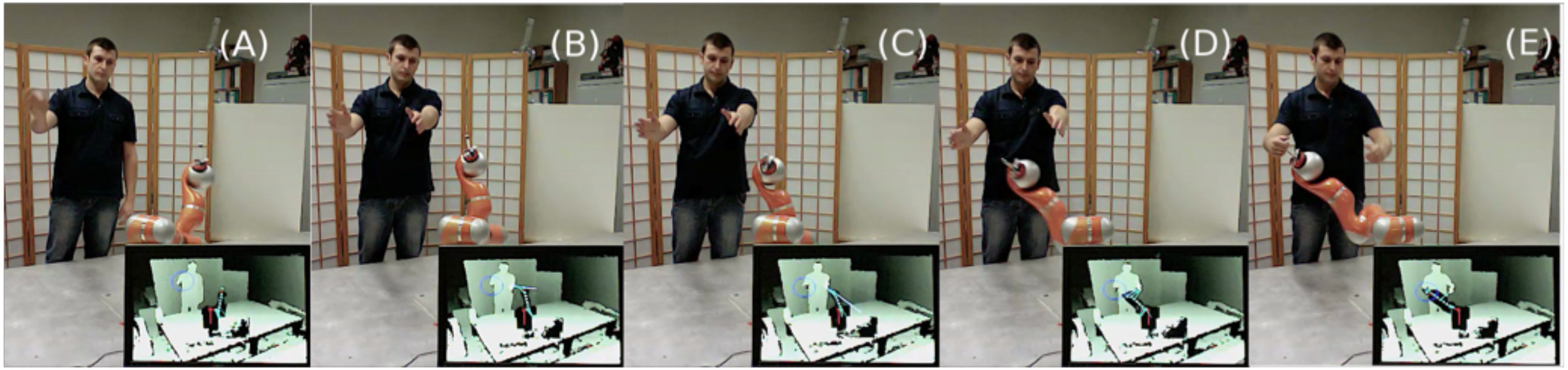

A control architecture for physical HRI

Relation with ISO Standard 10218 and Technical Specification 15066

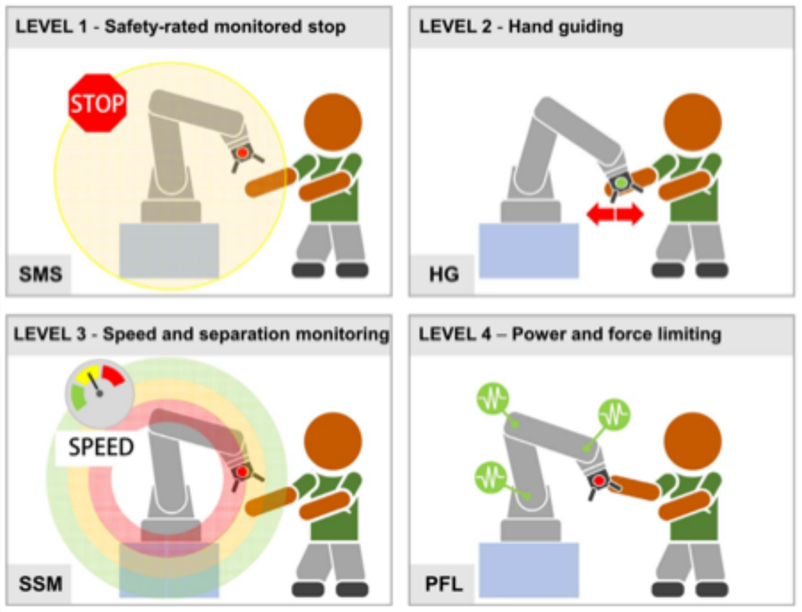

SAFETY	Speed	Separation distance	Torques	Operator controls	Main risk reduction
Safety-rated monitored stop COEXISTENCE	Zero while operator in CWS	Small or zero	Gravity + load compensation only	None while operator in CWS	No motion in presence of operator
Hand guiding COLLABORATION	Safety-rated monitored speed	Small or zero	As by direct operator input	E-stop; Enabling device; Motion input	Motion only by direct operator input
Speed and separation monitoring COEXISTENCE	Safety-rated monitored speed	Safety-rated monitored distance	As required to execute application and maintain min separation distance	None while operator in CWS	Contact between robot and operator prevented
Power and force limiting COLLABORATION	Max determined by RA to limit impact forces	Small or zero	Max determined by RA to limit static forces	As required by application	By design or control, robot cannot impart excessive force

ISO 10218-1/2:2011
ISO/TS 15066:2016

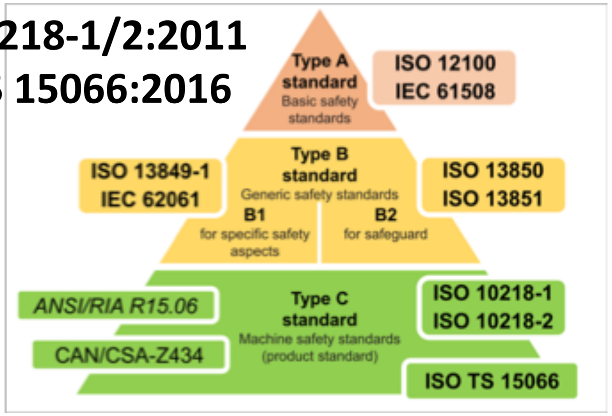

- collision detection and reaction
- workspace sharing
  – with collision avoidance
- coordinated motions & actions
  – with/without contact

Collision event pipeline

Haddadin, De Luca, Albu-Schäffer (T-RO 2015)

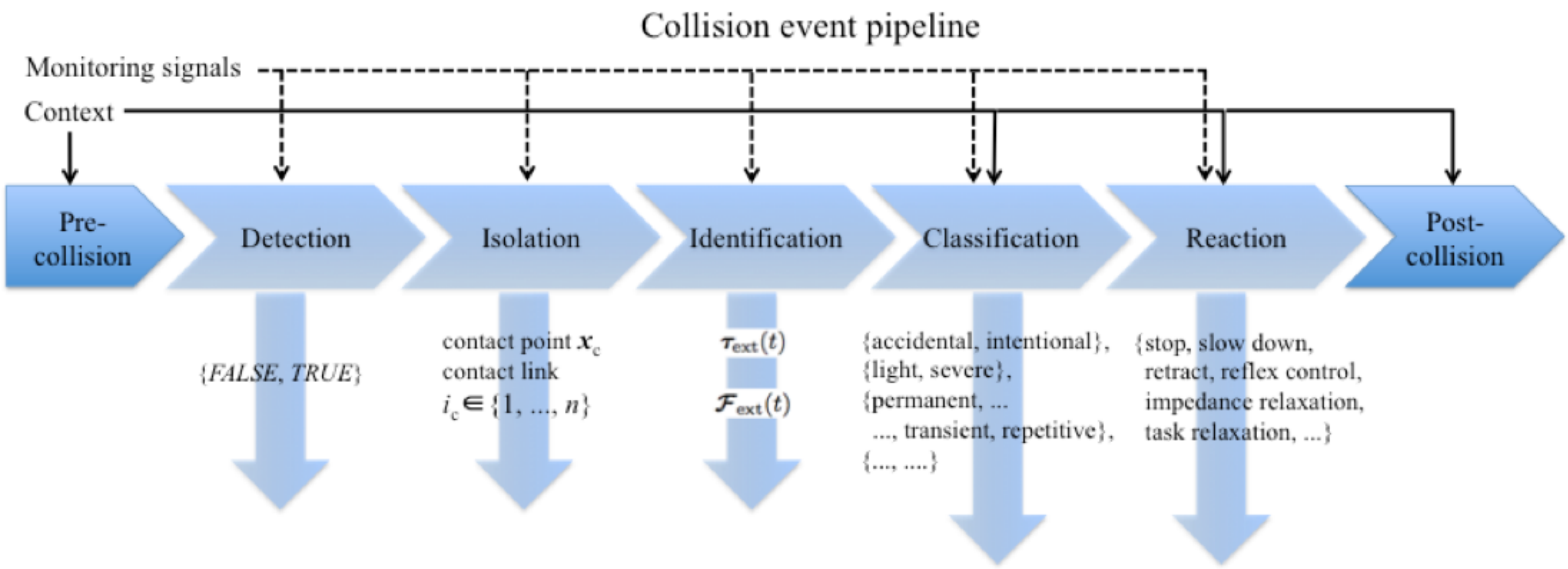

Monitoring signals can be generated from sensors or models (signal- or model-based methods)

Context information is needed (or useful) to take the right or most suitable decisions

Monitoring robot collisions

Applies equally to rigid and elastic joints, with and without joint torque sensing

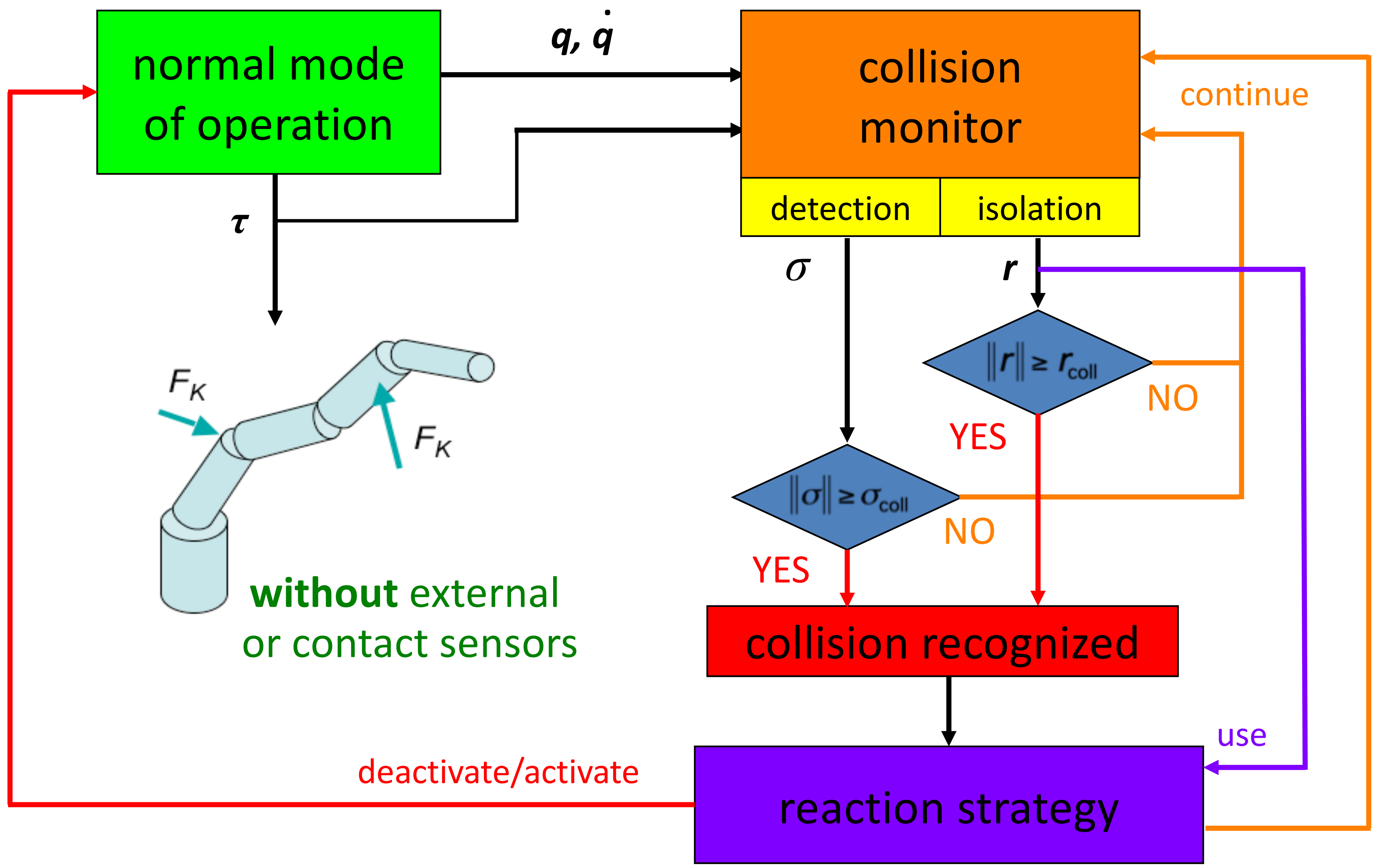

Energy-based residual

Block diagram for the generator of a scalar residual signal

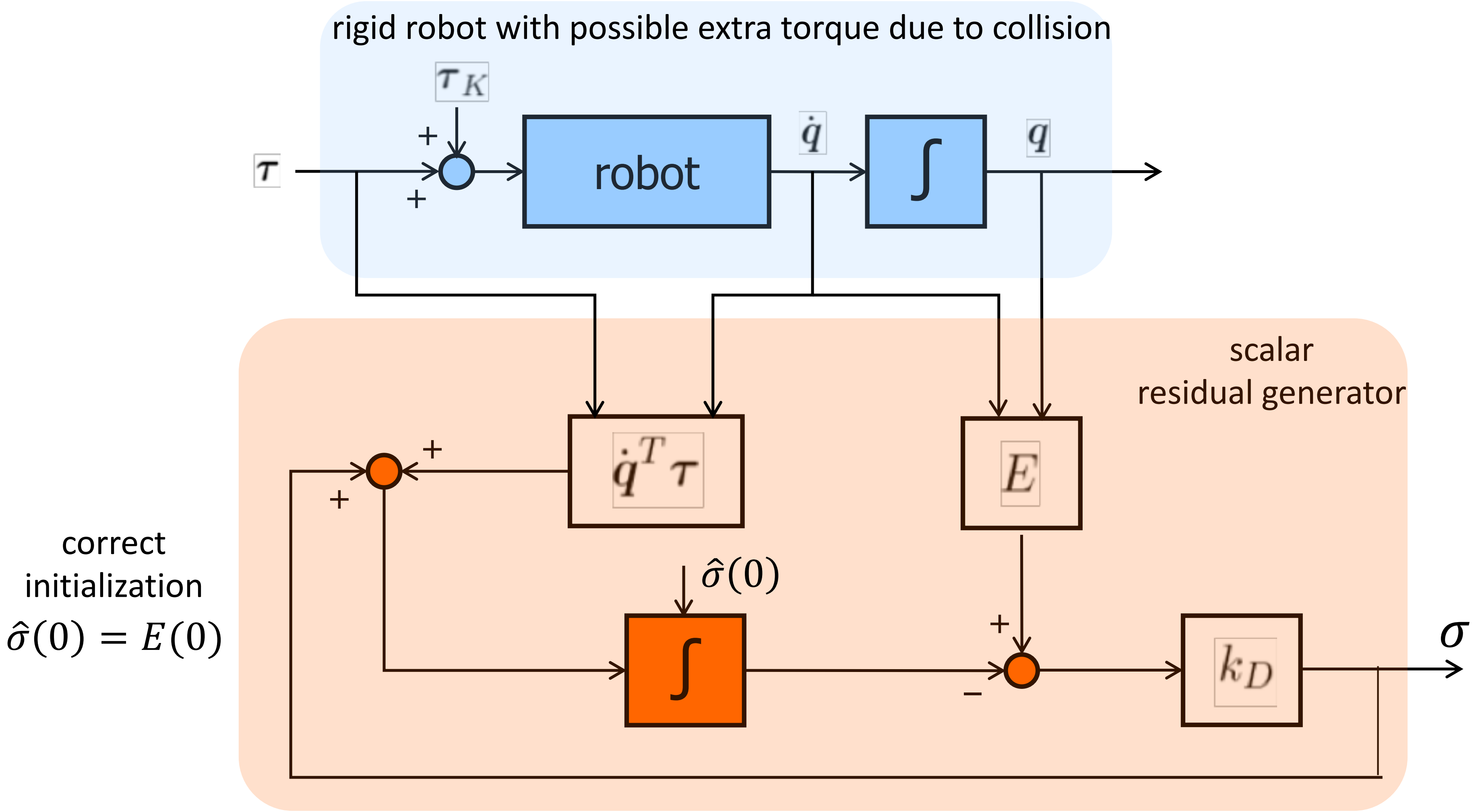

$$\sigma(t) = k_D \left[E(t) - \int_0^t (\dot{\boldsymbol{q}}^T \boldsymbol{\tau} + \sigma) ds - E(0) \right] \quad \Rightarrow \quad \dot{\sigma} = -k_D \, \sigma + k_D \, \dot{\boldsymbol{q}}^T \boldsymbol{\tau}_K$$

Collision detection

Experiment on a 6R robot with energy-based scalar residual

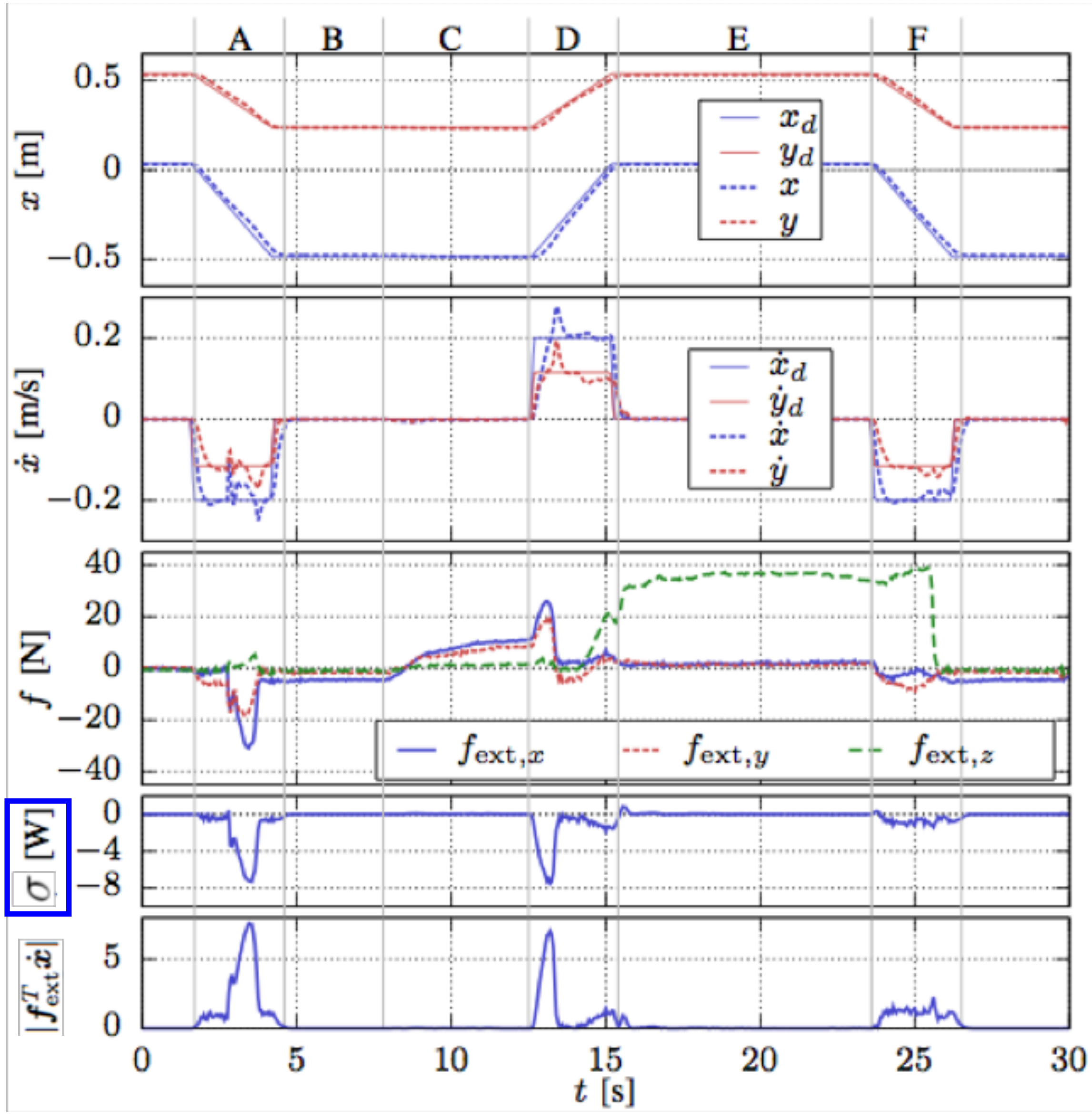

robot at rest or moving
under Cartesian impedance control
on a straight horizontal line
(with a F/T sensor at wrist for analysis)

6 phases

A: contact force applied is acting against motion direction ⇒ detection

B: no force applied, with robot at rest

C: force increases gradually, but robot is at rest ⇒ no detection

D: robot starts moving again, with force being applied ⇒ detection

E: robot stands still and a strong force is applied in z-direction ⇒ no detection

F: robot moves, with a z-force applied ≈ orthogonal to motion direction ⇒ poor detection

Momentum-based residual

Block diagram for the generator of a **vector** residual signal

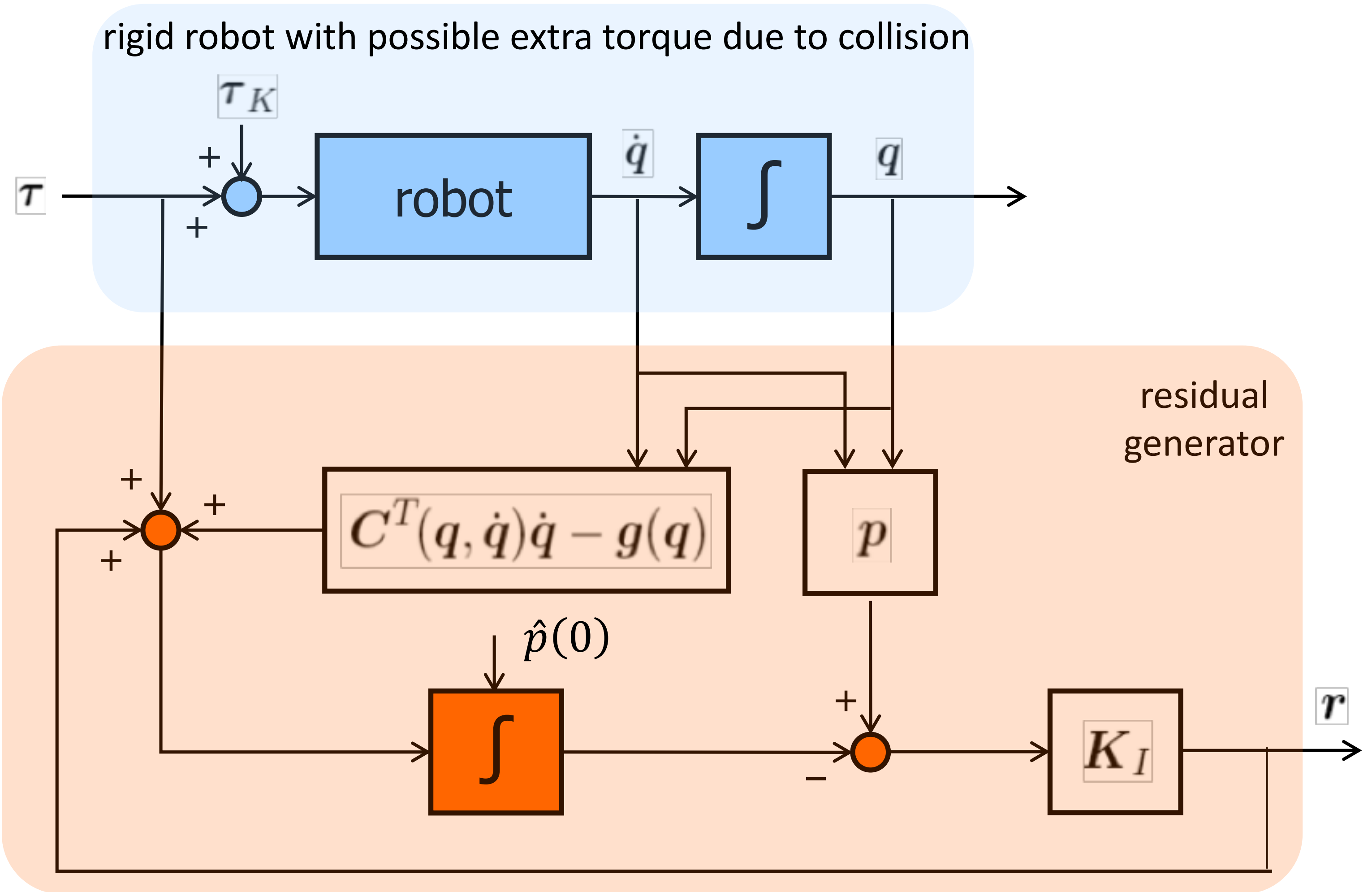

correct initialization
$\hat{p}(0) = p(0)$

$$r(t) = K_I \left[p(t) - \int_0^t \left(\tau + C^T(q,\dot{q})\dot{q} - g(q) + r \right) ds - p(0) \right] \Rightarrow \dot{r} = -K_I r + K_I \tau_K$$

Collision detection and isolation

Based on **residuals** for robots with rigid or **elastic joints** (ICRA 2005, IROS 2006)

- dynamic model of robots with elastic joints and environment interaction

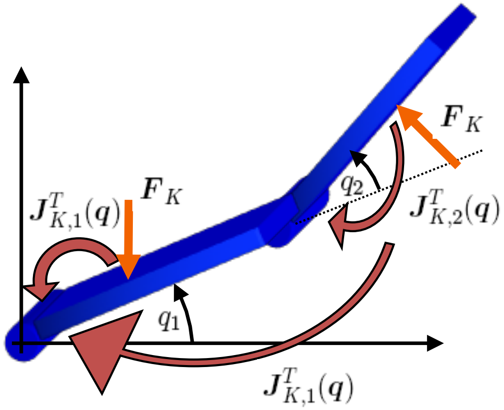

$$M(q)\ddot{q} + C(q,\dot{q})\dot{q} + g(q) = \tau_J + \tau_K$$

joint torque due to link collision

$$\tau_K = J_K^T(q) F_K$$

$$B\ddot{\theta} + \tau_J = \tau$$

motor torques commands

elastic torques at the joints

$$\tau_J = K(\theta - q)$$

- DLR LWR-III robot with multiple joint sensors
  - **encoders** for motor (θ) and link (q) positions
  - joint **torque sensor** for τ_J

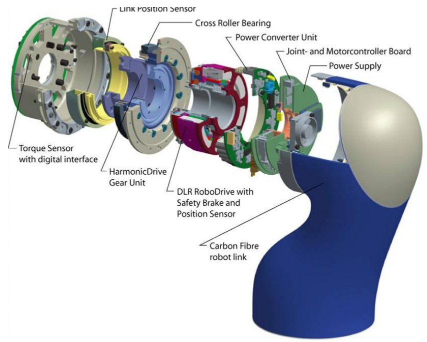

monitoring signal:
(link) momentum-based residual vector

$$\boxed{r = K_I \left(M(q)\dot{q} - \int_0^t \left(\tau_J + C^T(q,\dot{q})\dot{q} - g(q) + r \right) ds \right)}$$

$K_I > 0$ (diagonal and large) ➡ $\dot{r} = -K_I r + K_I \tau_K$

$r \approx \tau_K$ **detection** (over a threshold)

$$r = [\, * \quad \ldots \quad * \quad * \quad \underset{i+1}{0} \quad \underset{\ldots}{\ldots} \quad \underset{N}{0} \,]^T$$

isolation (collision at link i)

Collision detection and isolation

Experiment on 3 links of a position-controlled LWR-III with **momentum-based vector** signal

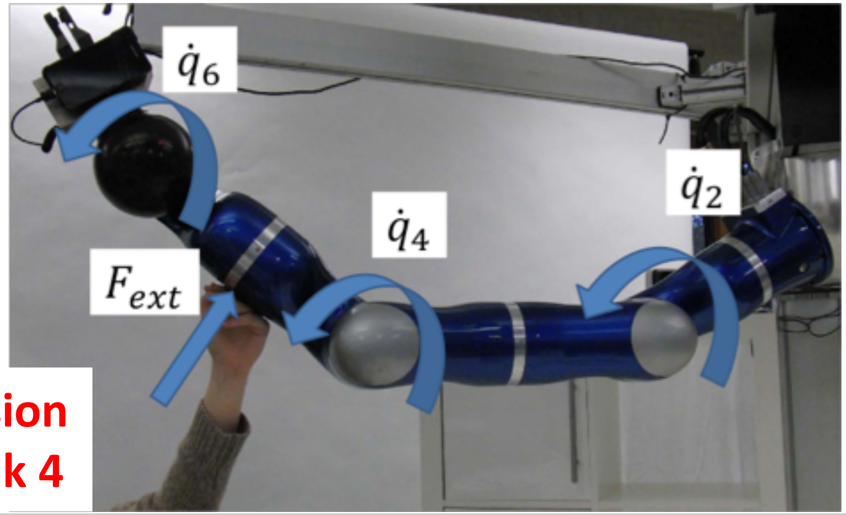

collision at link 4

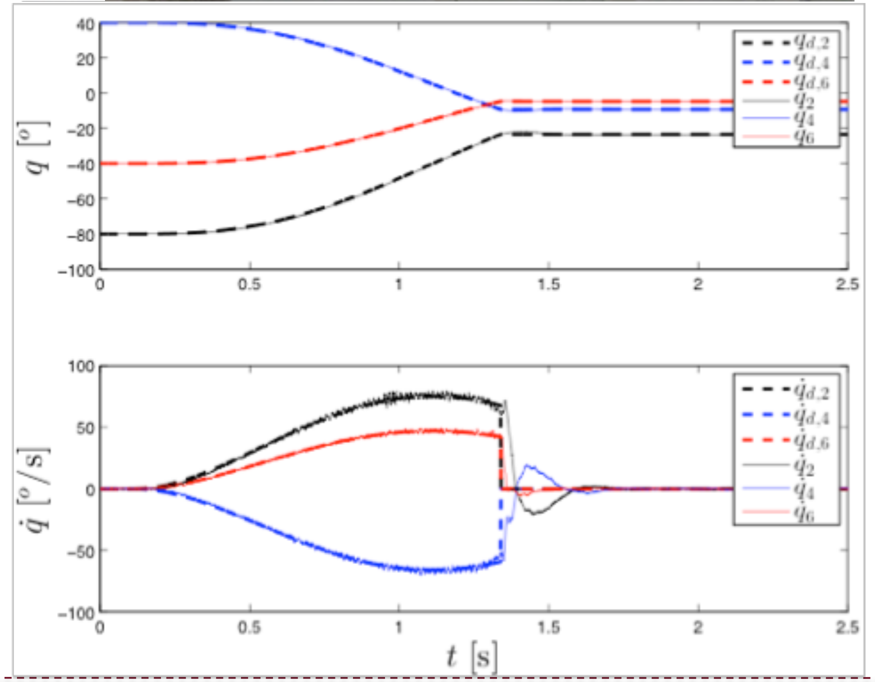

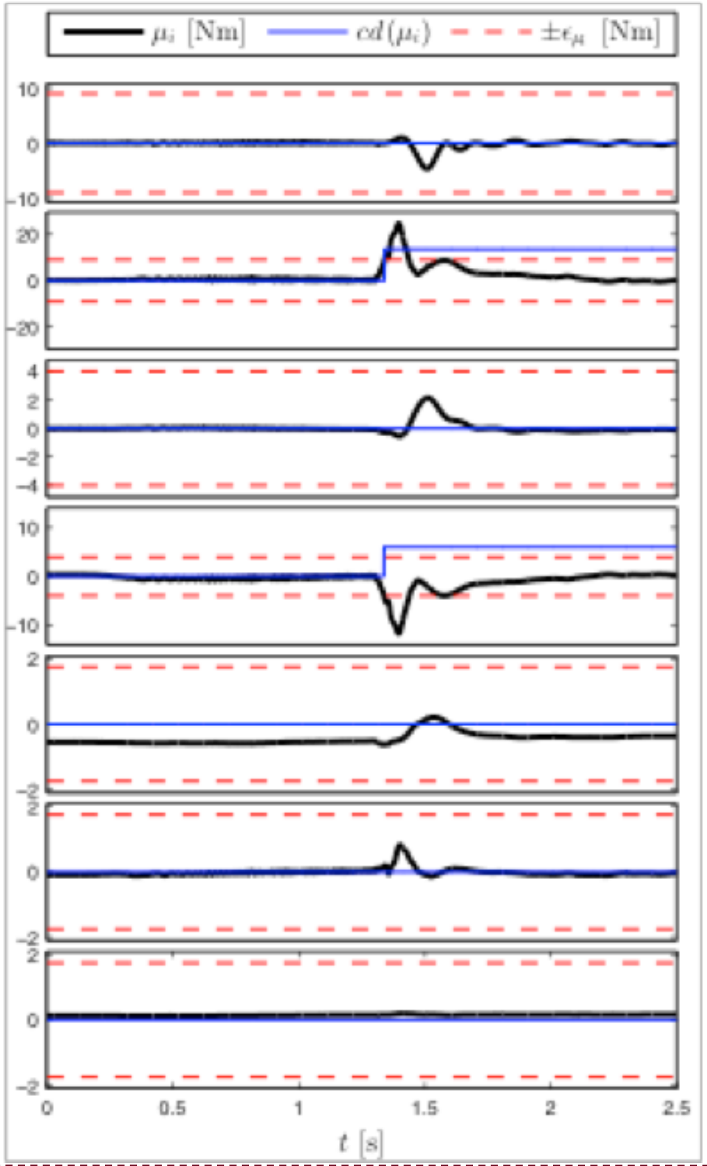

cd_2 = ON

cd_4 = ON

Detection time delay

Experiment with a dummy head instrumented with an accelerometer

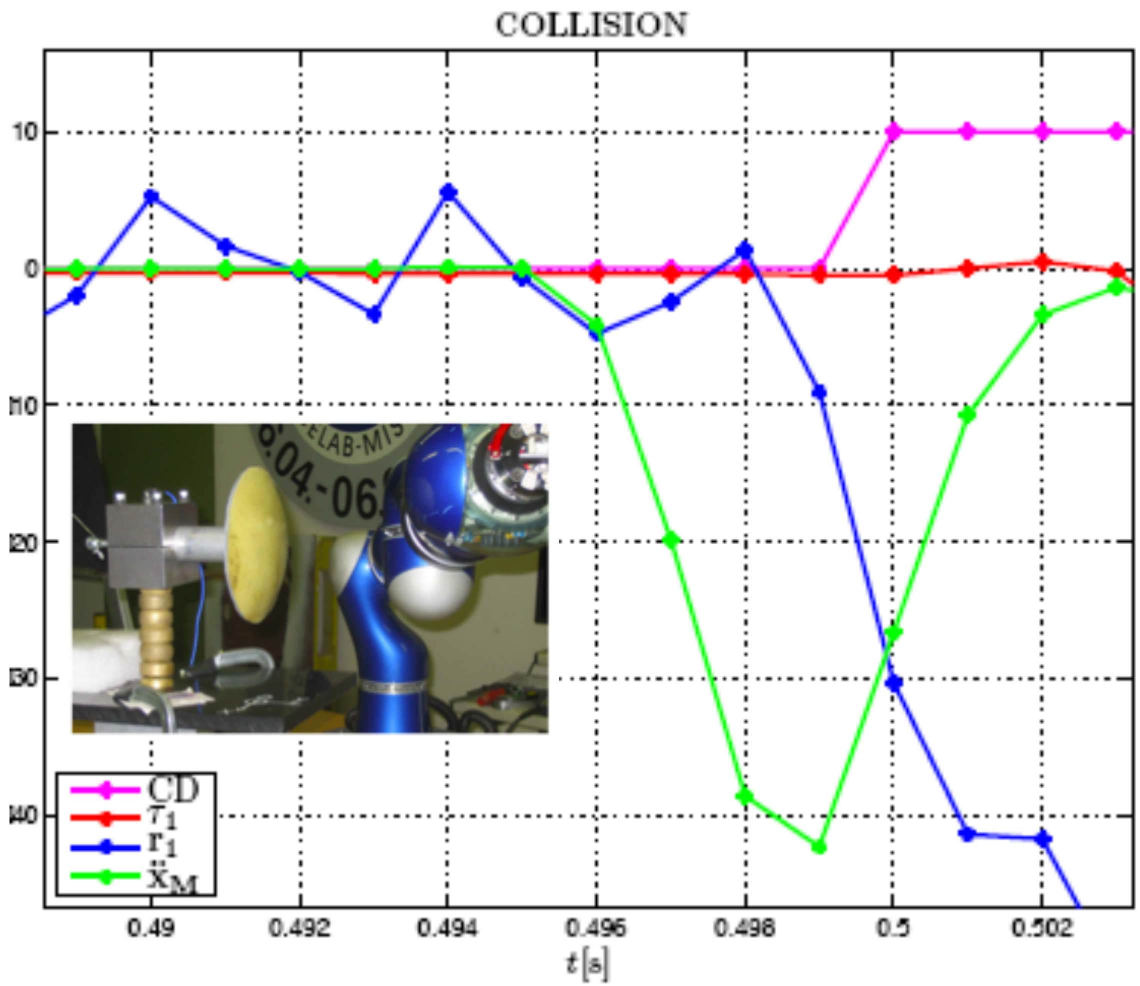

2-4 msec!

impact with the dummy head

measured (elastic) joint torque

residual r_1

0/1 index for detection

dummy head acceleration

gain K_I = diag{25}

threshold = 5-10% of max rated torque

Collision reaction

Using the vector residual

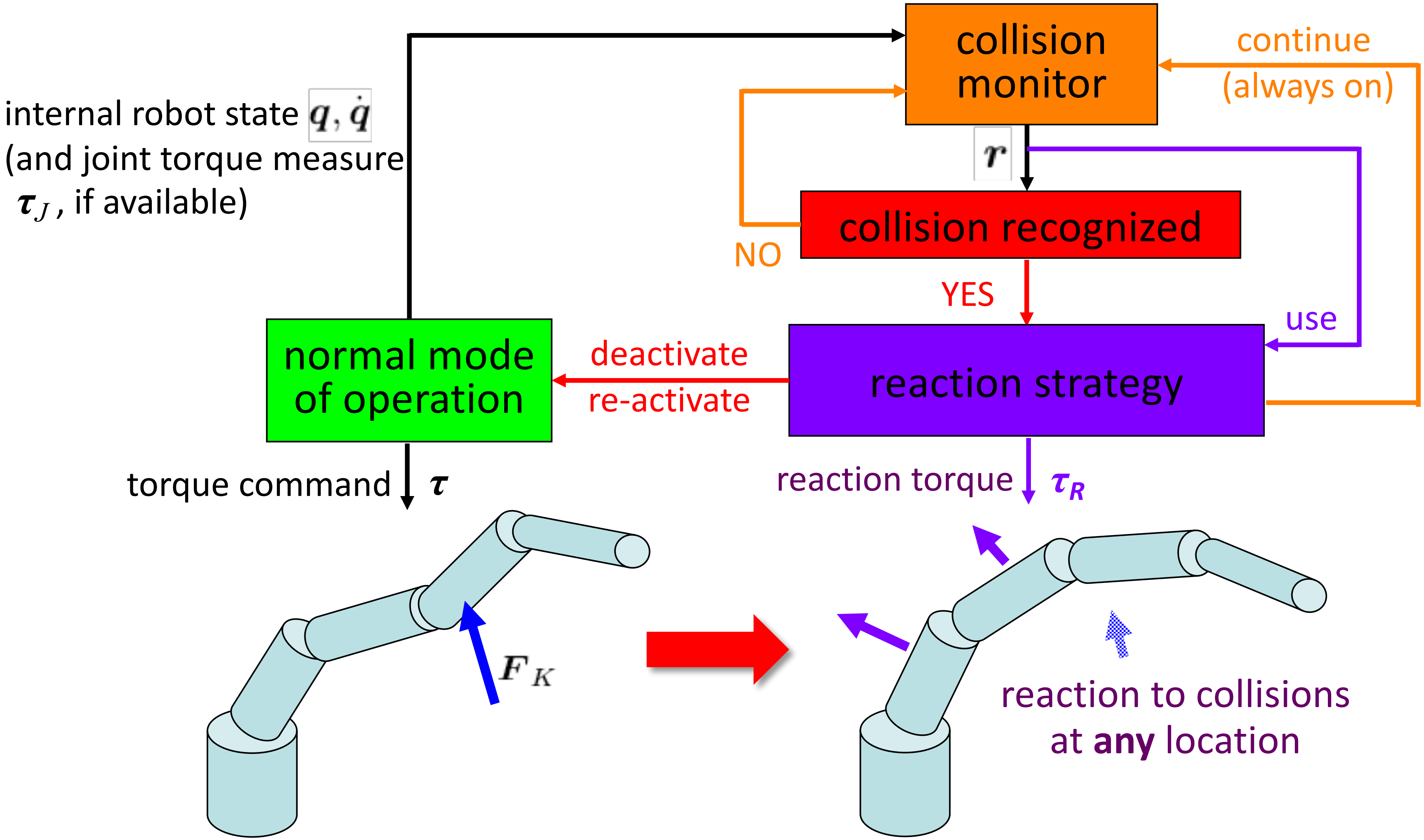

Collision detection and reaction

Residual-based experiments on DLR LWR-III (IROS 2006)

- collision detection followed by different reaction strategies
- zero-gravity behavior: gravity is always compensated first (by control)
- detection time: 2 ms, reaction time: + 1 ms

admittance mode	reflex torque	reflex torque
first impact at 60°/s		first impact at 90°/s
$\dot{\boldsymbol{q}}_r = \boldsymbol{K}_Q \boldsymbol{r}$	$\boldsymbol{\tau} = \boldsymbol{K}_R \boldsymbol{r}$	

Collision reaction

Portfolio of possible robot reactions

residual amplitude ∝ severity level of collision

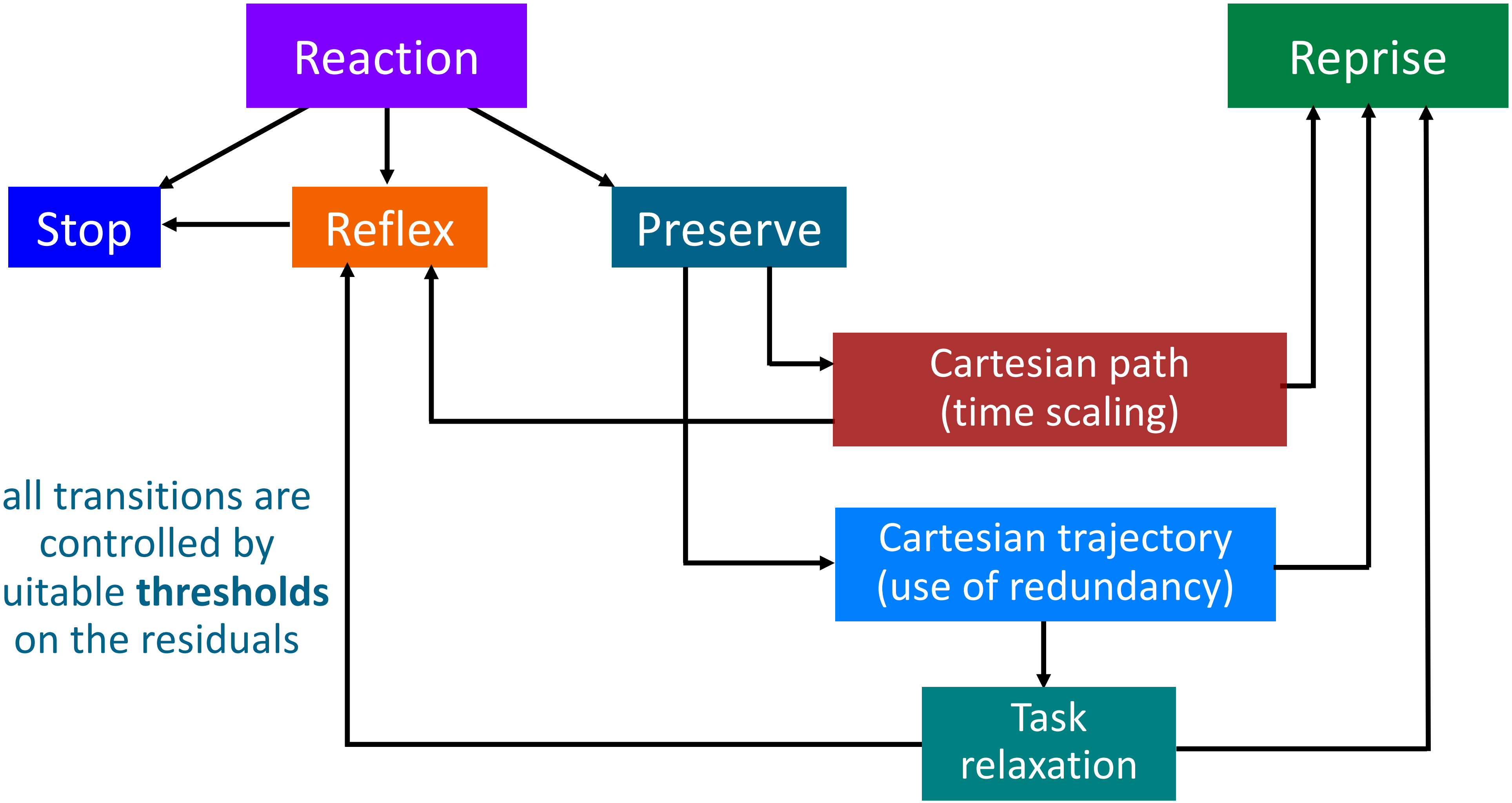

all transitions are controlled by suitable **thresholds** on the residuals

Collision reaction

Further examples (IROS 2008)

- without external sensing
- any place, any time ...

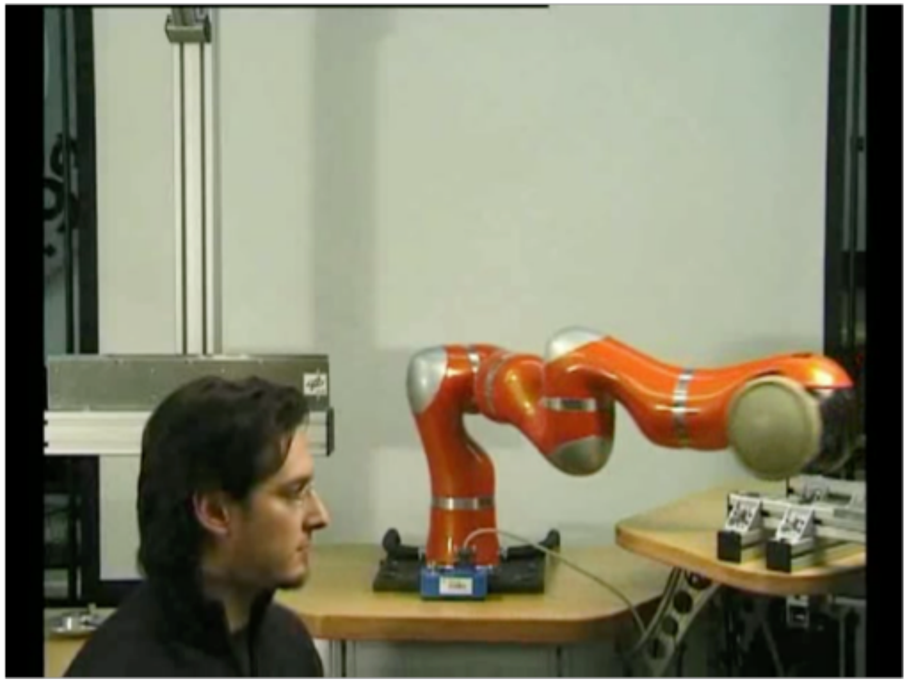

- the famous "volunteer" Sami Haddadin (now a "big" professor)

- manipulator is position-controlled on a geometric path
- timing slows down, stops, possibly reverses

Sensitivity to payload changes/uncertainty

Collision detection and isolation after few moves for identification (IROS 2017)

residuals with online estimated
payload after 10 positioning

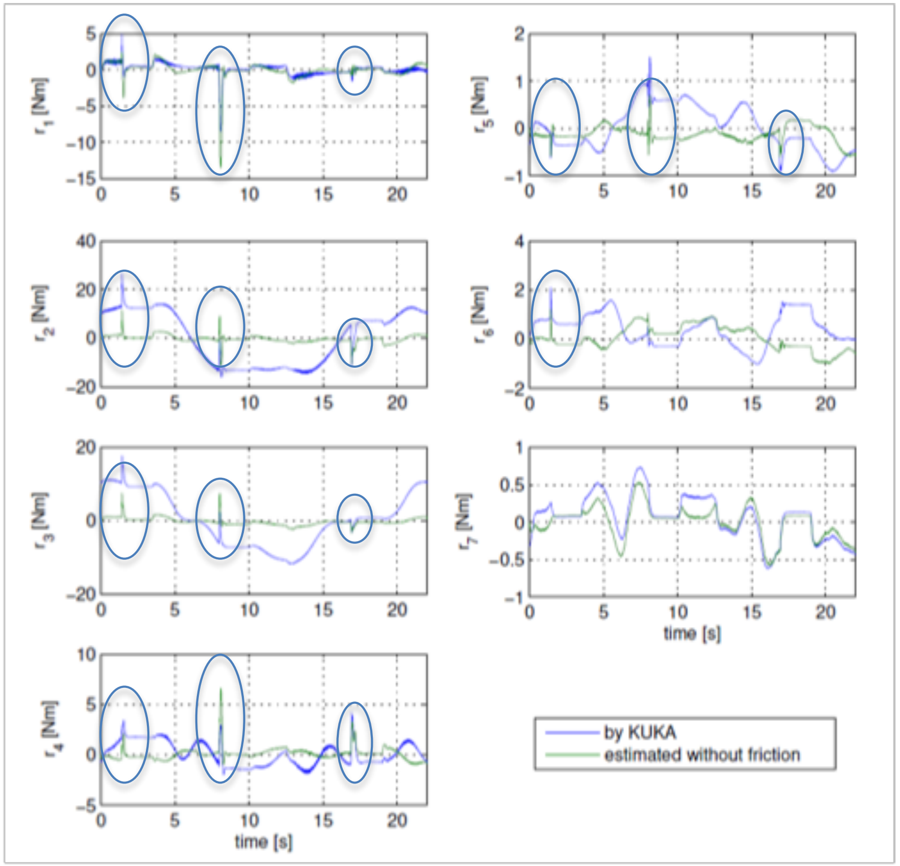

all three collisions are detected by our residual
when exceeding the threshold of 6 Nm

https://youtu.be/fNP6smdp7aE

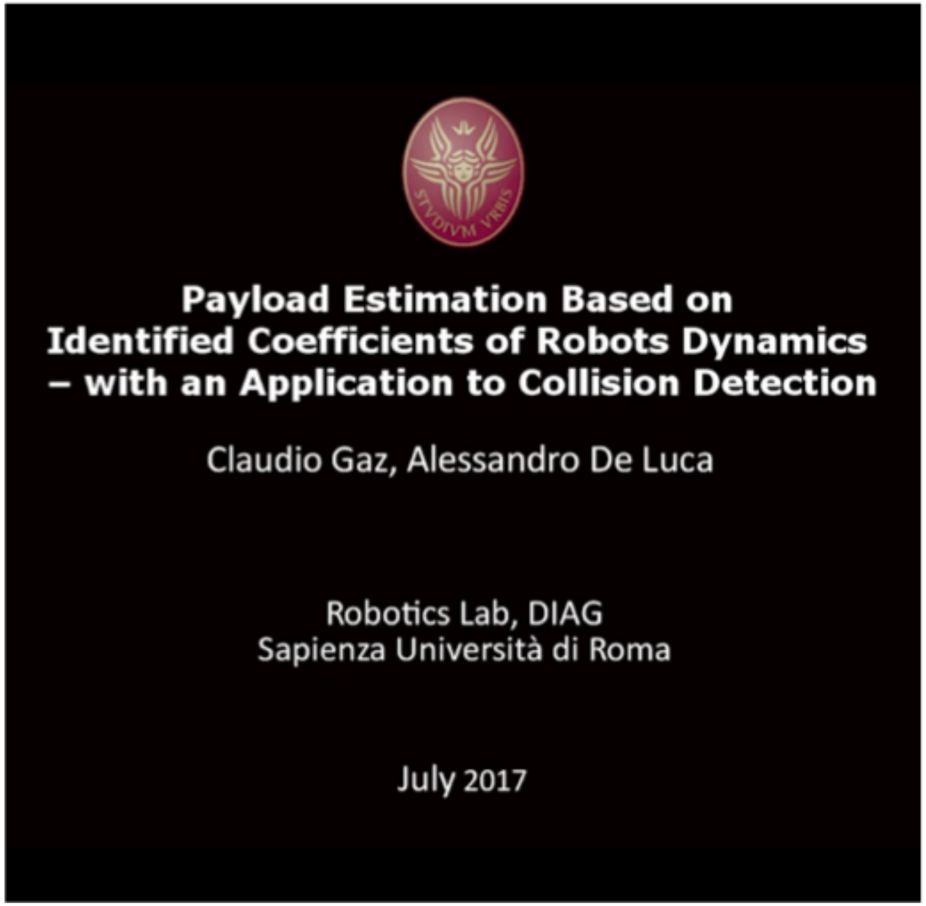

Collision avoidance

Using exteroceptive sensors to monitor robot workspace (ICRA 2010)

- **external sensing:** stereo-camera, TOF, structured light, **RGB-Depth**, laser, presence, ... placed optimally to minimize occlusions (robot is to be removed from images)

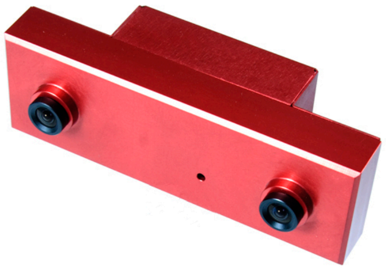

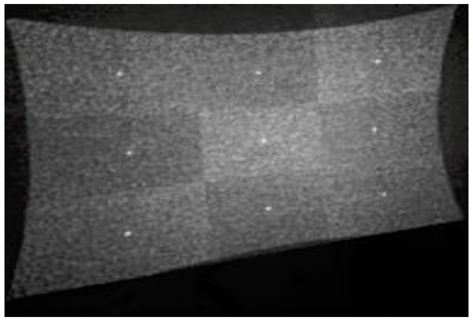

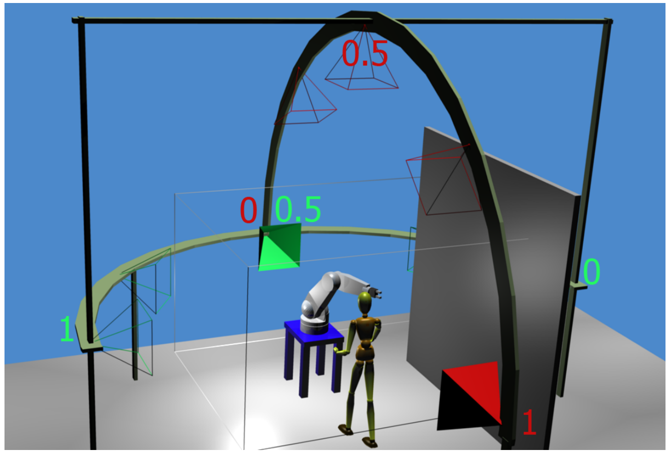

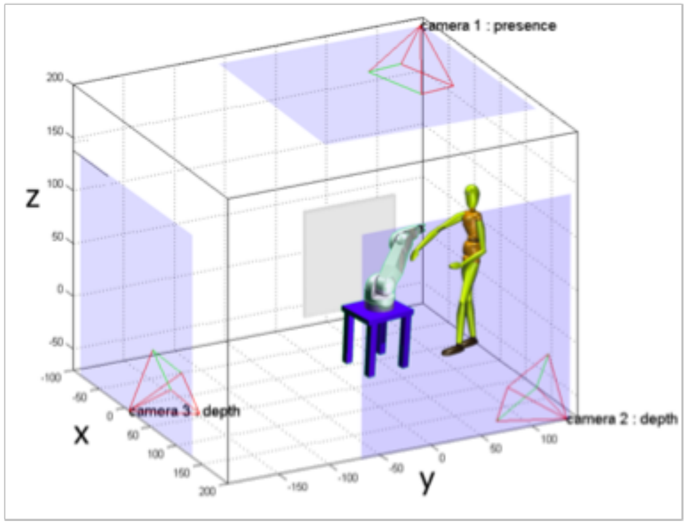

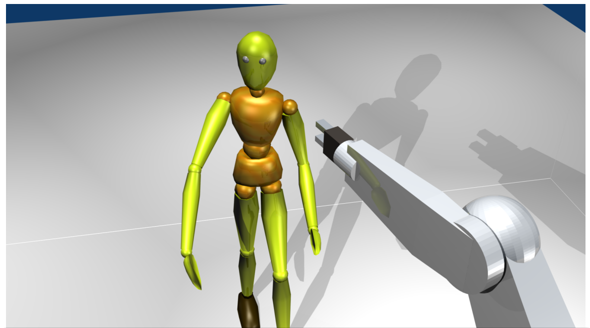

Depth image

How to use it?

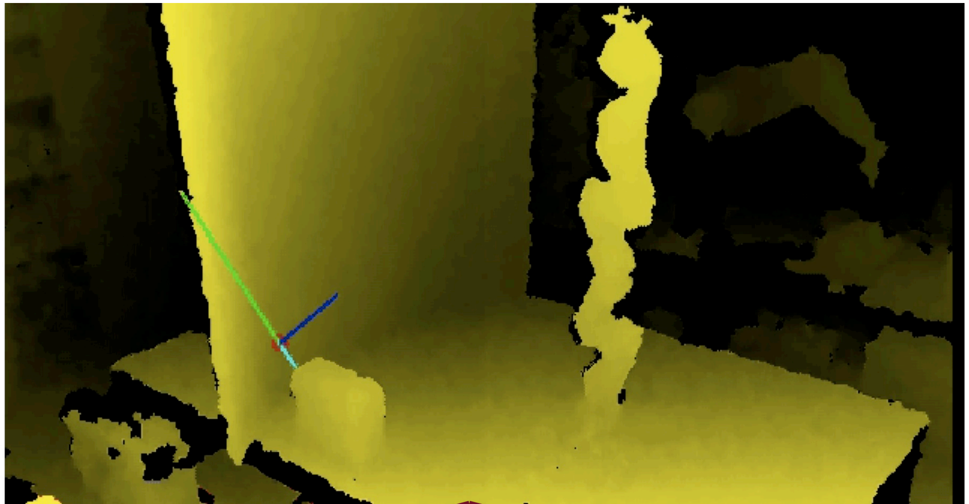

Configuration Space

Depth Space

Cartesian Space

Depth space

2 ½ space for efficient robot-obstacle distance computations (ICRA 2012)

$$
\begin{aligned}
p_x &= \frac{x_C f s_x}{z_C} + c_x \\
p_y &= \frac{y_C f s_y}{z_C} + c_y \\
d_p &= z_C
\end{aligned}
$$

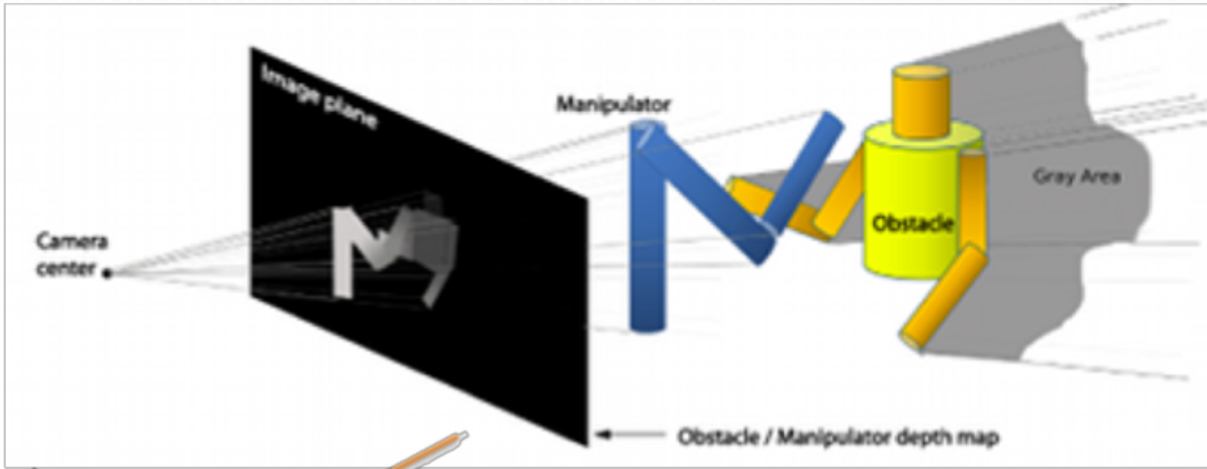

no 3D-Cartesian reconstruction or models
no need to use Point Cloud Library (PCL)

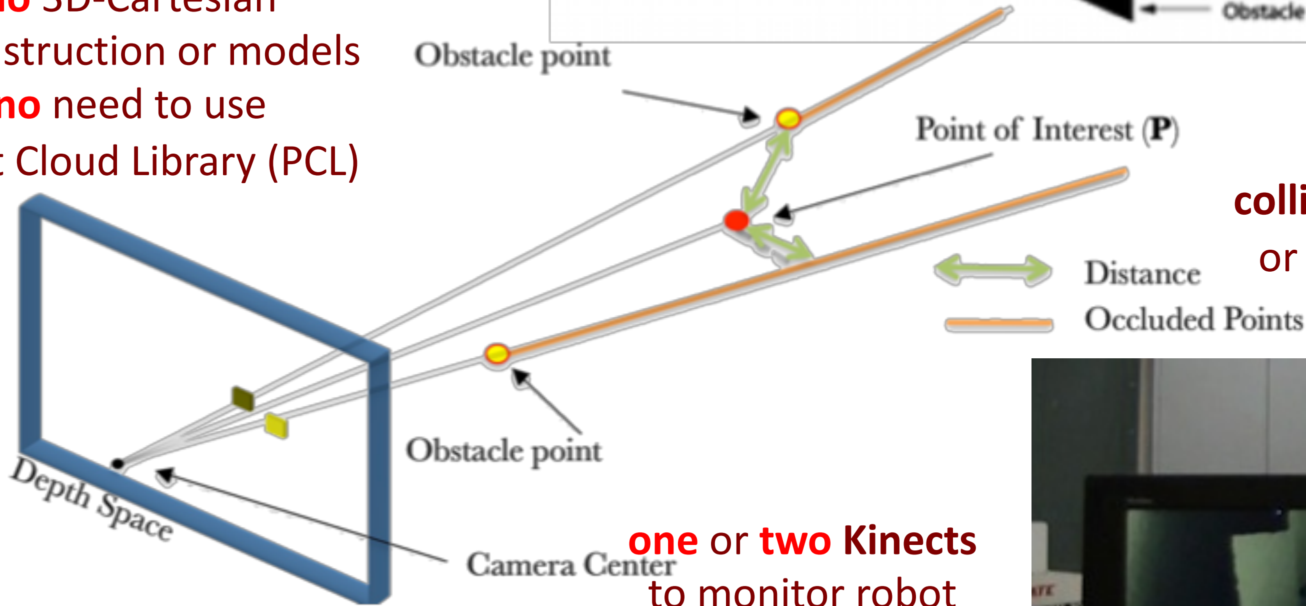

use distance, e.g., with artificial potentials, for **collision avoidance** during motion or **to slow down/stop** the robot

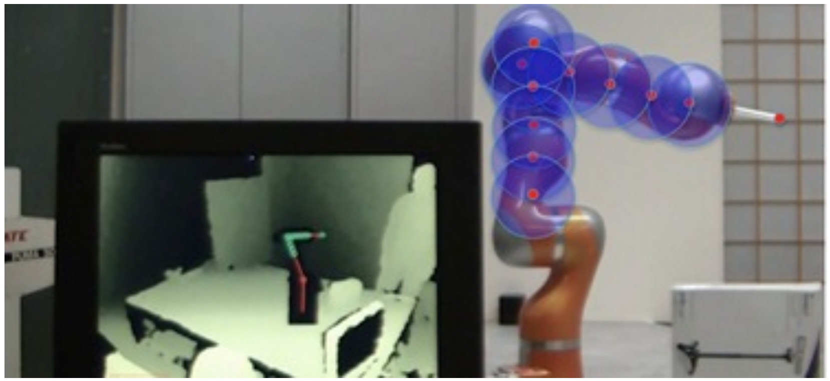

one or **two Kinects** to monitor robot workspace **@ 300 Hz** with minimal gray areas

see also the video https://youtu.be/iapfbAfklw4

Distance and contact point localization

Using the depth sensor

- Localization of contact point
  - depth image of the environment captured by a Kinect sensor
  - robot is removed from image with a URDF filter[1], starting from its 3D CAD model
  - tracking of the **human hands** (later, of the whole body), using the filtered image
  - each link surface of the robot is modelled with a set of polygonal primitive shapes
  - distance between the hand and all the vertices of the polygons is computed
  - when contact is detected, the vertex at minimum distance will be identified as the contact point
  - algorithm is applied in parallel to both left and right hands

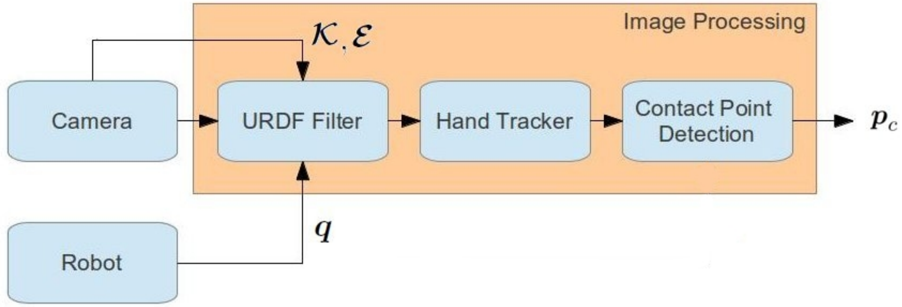

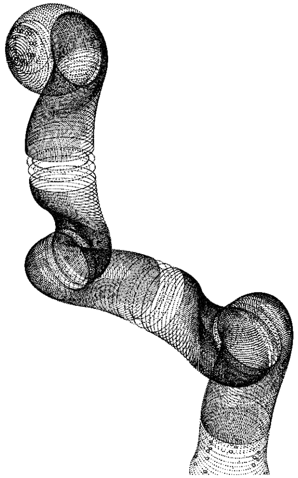

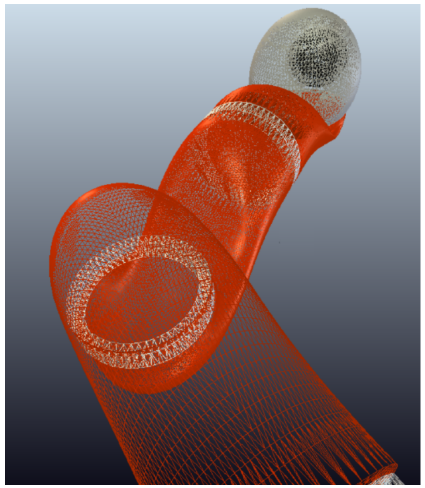

1. by TUM, available at http://github.com/blodow/realtime_urdf_filter

Safe physical human-robot collaboration

Excerpts from a long video at IROS 2013

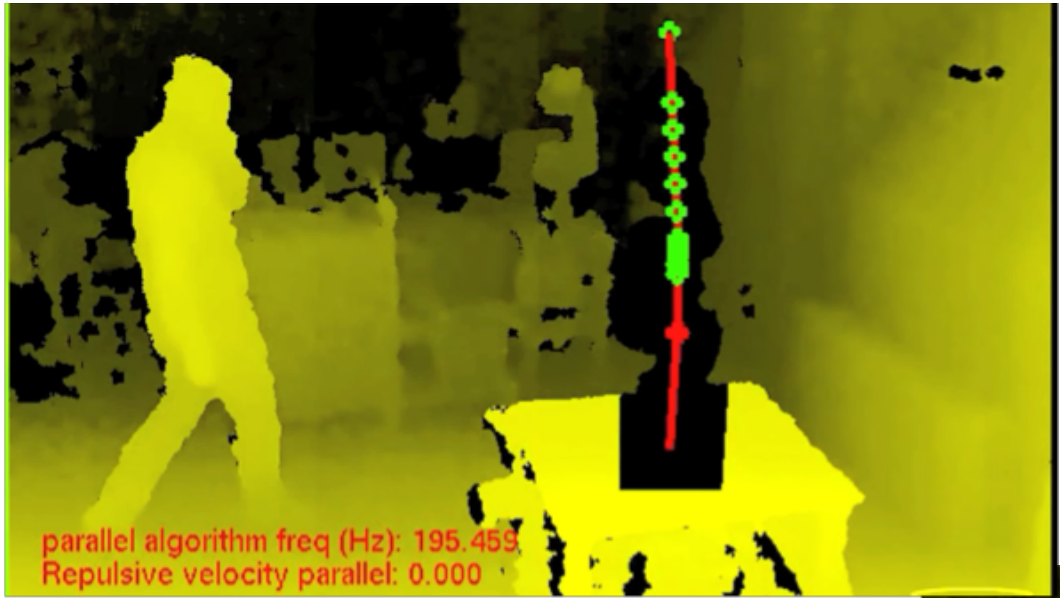

coexistence through collision avoidance

https://youtu.be/pIlhY8E3HFg

collaboration through contact identification (here, end-effector only)

Distance and contact estimation

Using Kinect, CAD model, distance computation, and residual to localize contact

- when the residual indicates a contact/collision (and colliding link), the **vertex** in the robot CAD surface model **with minimum distance** is taken as the contact point
- algorithm is applied in parallel to both left and right hand (or other body parts)

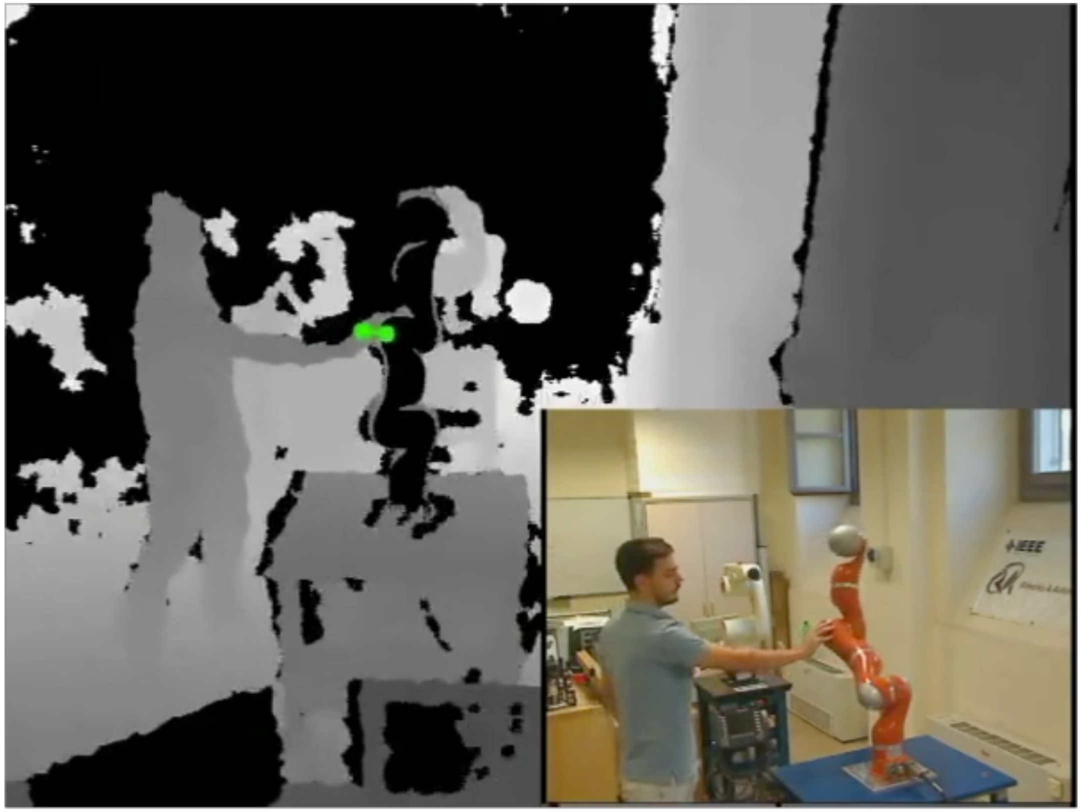

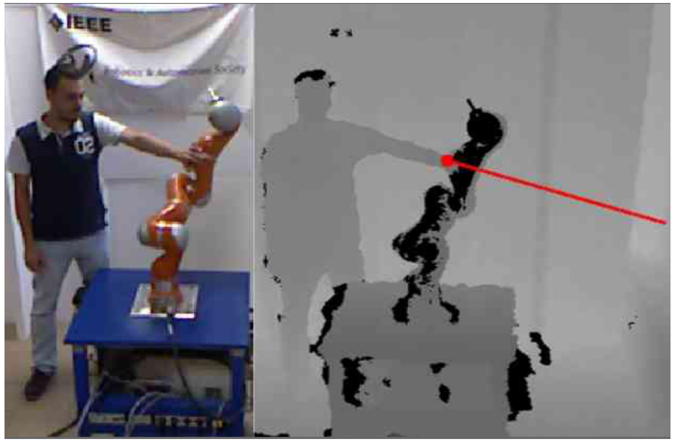

Monitoring the workspace with two Kinects

…without giving away the depth space computational approach (RA-L 2016)

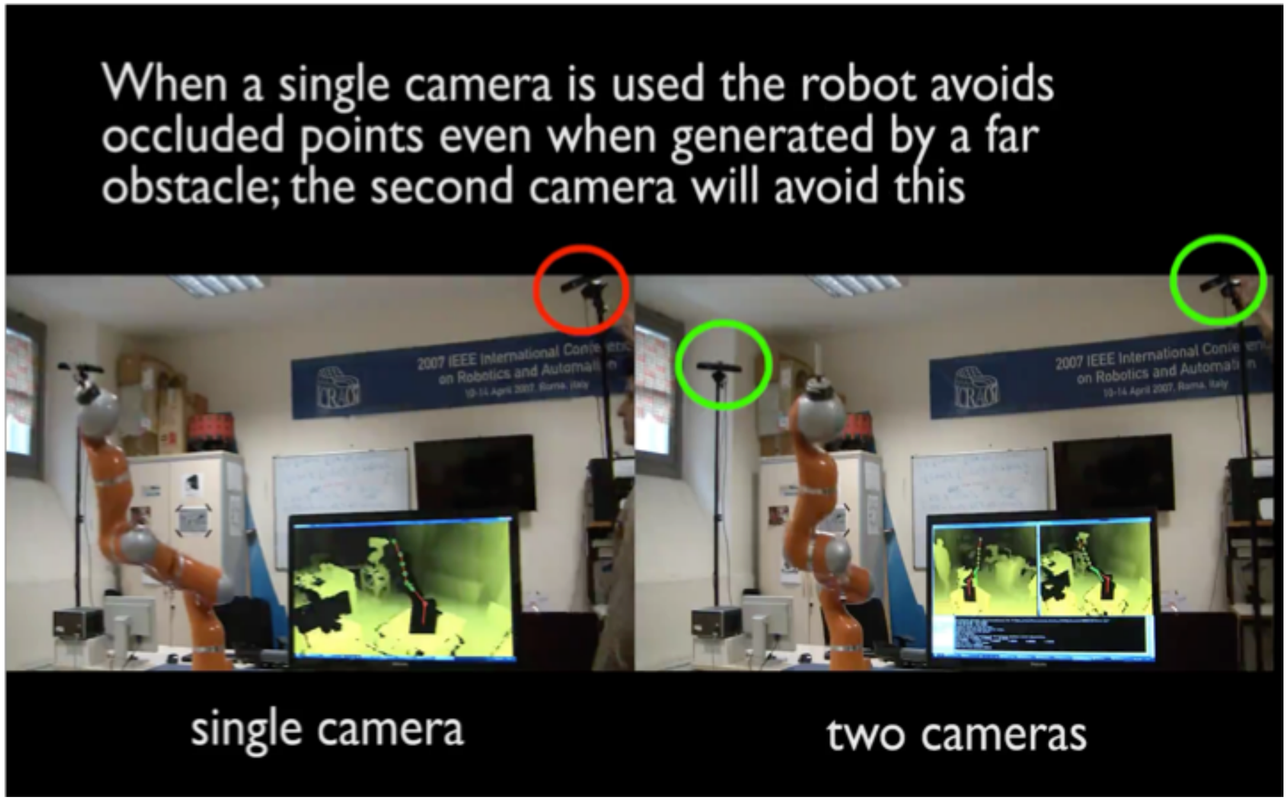

https://youtu.be/WIw_Uj_ooYI

real-time efficiency
extremely fast also with 2 devices: 300 Hz rate (RGB-D camera has 30 fps)

problems solved by the second camera

+ eliminates collision with false, far away "shadow" obstacles
+ reduces to a minimum gray areas, thus detects what is "behind" the robot
+ calibration is done off-line

CAD model of the robot and equipments/tools/cables

Filtering out the right parts from the depth images

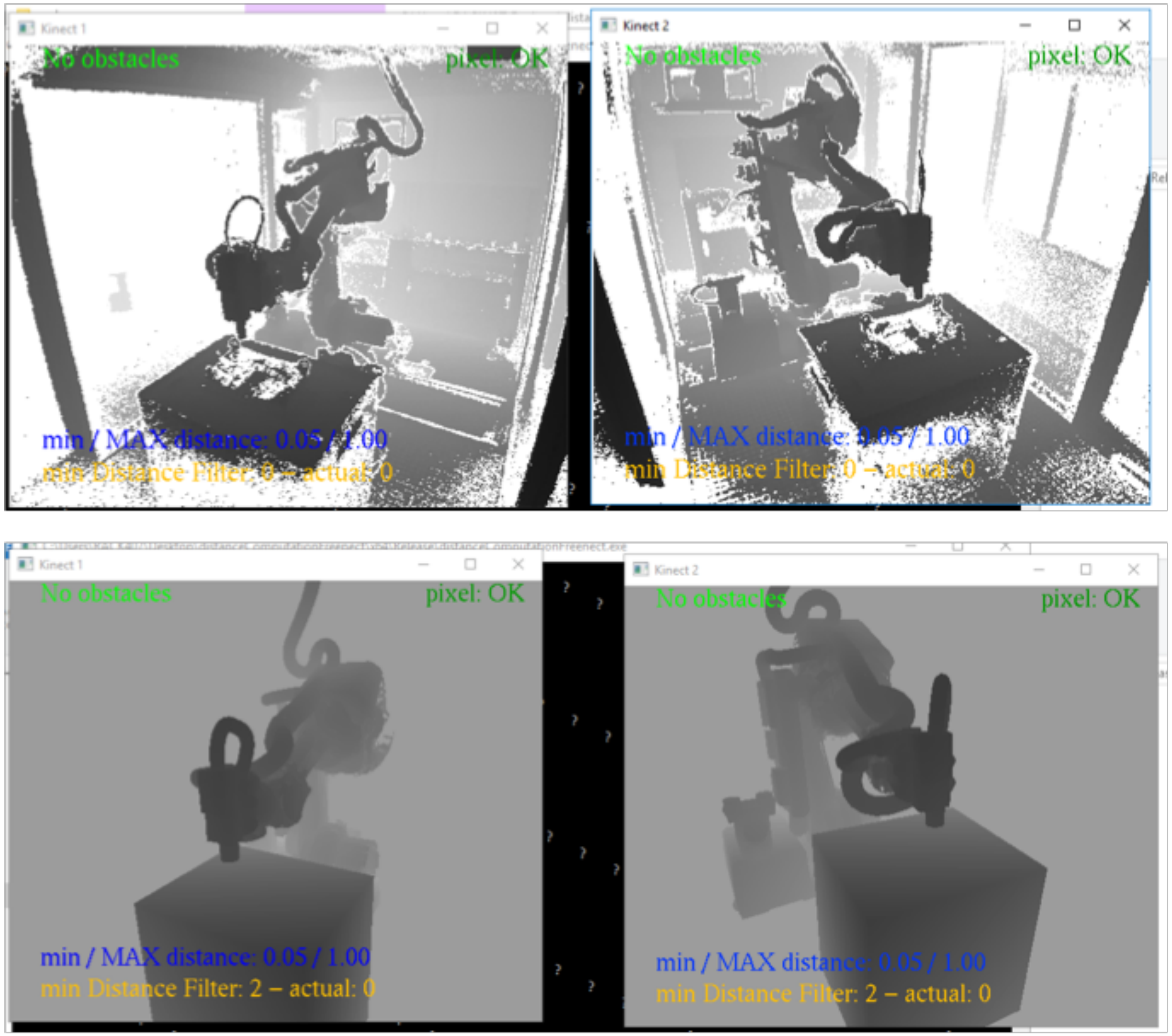

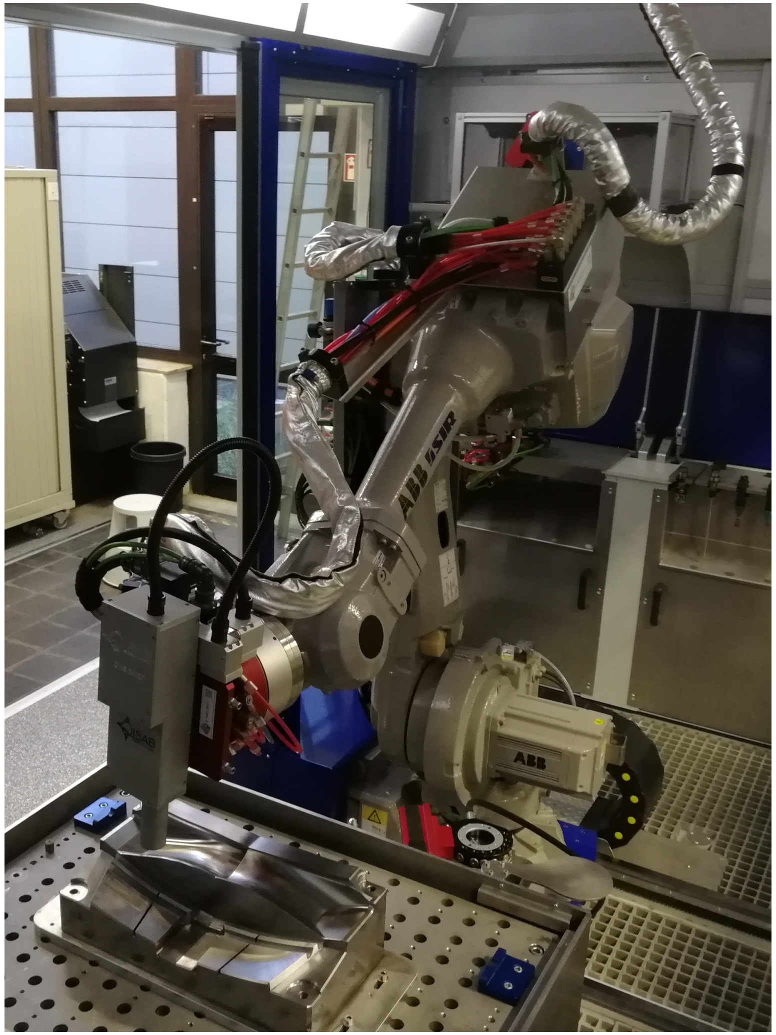

Contact point localization

CUDA framework (IROS 2017)

Real-time contact point localization

- the algorithm is based on distance computation in depth space, taking advantage from a **CUDA framework** for massively parallel **GPU** programming
- processing of three 2.5D images:
  - real depth image I_r , captured by a RGB-D sensor (a Kinect)
  - virtual depth image I_v, containing only a projection of the robot CAD model
  - filtered depth image $I_f = f(I_r, I_v)$, containing only the obstacles

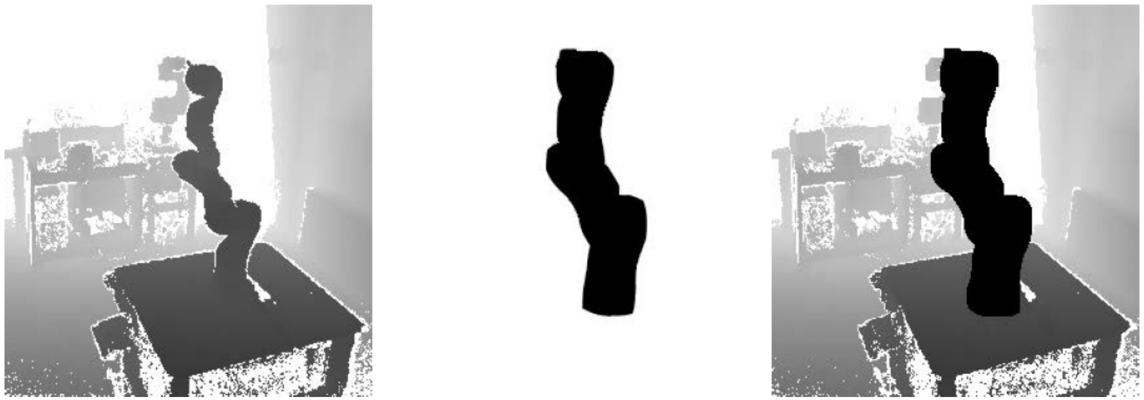

- **distance computation** (in depth space) between all robot points in the virtual depth image and all obstacle points in the filtered depth image

Contact point localization

Distance in depth space

- compute distances between all robot points $\boldsymbol{P}_D = \begin{pmatrix} p_{v,x} & p_{v,y} & d_v \end{pmatrix}^T$ in virtual depth image and all obstacles points $\boldsymbol{O}_D = \begin{pmatrix} p_{f,x} & p_{f,y} & d_f \end{pmatrix}^T$ in filtered depth image

$$d(\boldsymbol{O}, \boldsymbol{P}) = \sqrt{v_x^2 + v_y^2 + v_z^2}, \quad \text{with} \quad \begin{aligned} v_x &= \frac{(p_{f,x} - c_x)d_f - (p_{v,x} - c_x)d_v}{f\, s_x} \\ v_y &= \frac{(p_{f,y} - c_y)d_f - (p_{v,y} - c_y)d_v}{f\, s_y} \\ v_z &= d_f - d_v \end{aligned}$$

- when a contact is detected by the residual, the point of the visible robot surface at minimum distance from the obstacle is considered as contact point
- thanks to the parallel computing of the CUDA framework, the time needed to localize one or multiple contact points is the same

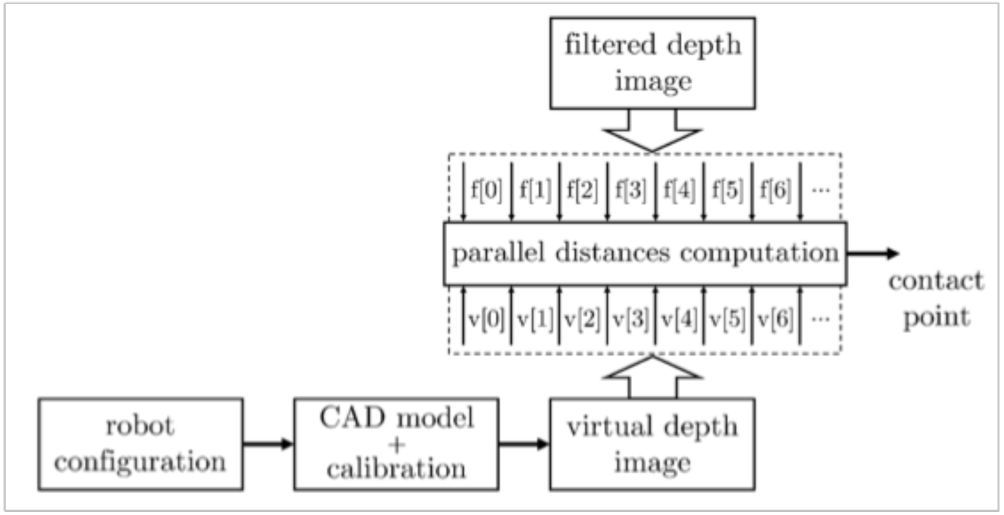

contact point localization processing

Safe coexistence in an industrial robotic cell

ABB IRB 4600 operation in an Abrasive Finishing cell with human access

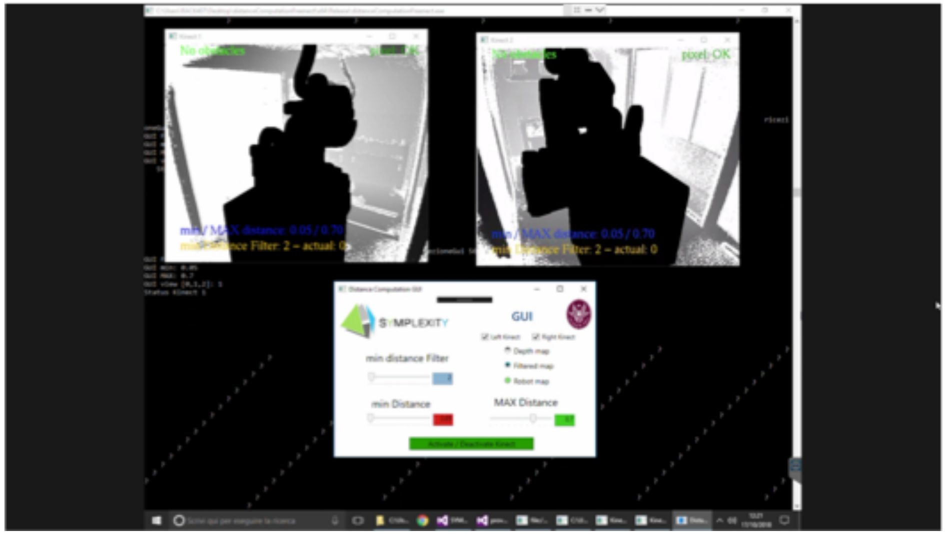

depth images and GUI

- robot is moving at max 100 mm/s
- no safety zones were defined in ABB SafeMove
- Kinect **OK** (except when the view of one of the cameras is obstructed on purpose)

SYMPLEXITY

Implemented control and communication architecture

Two **Kinects** for accurate HR distance monitoring, two **laser scanners** for backup safety

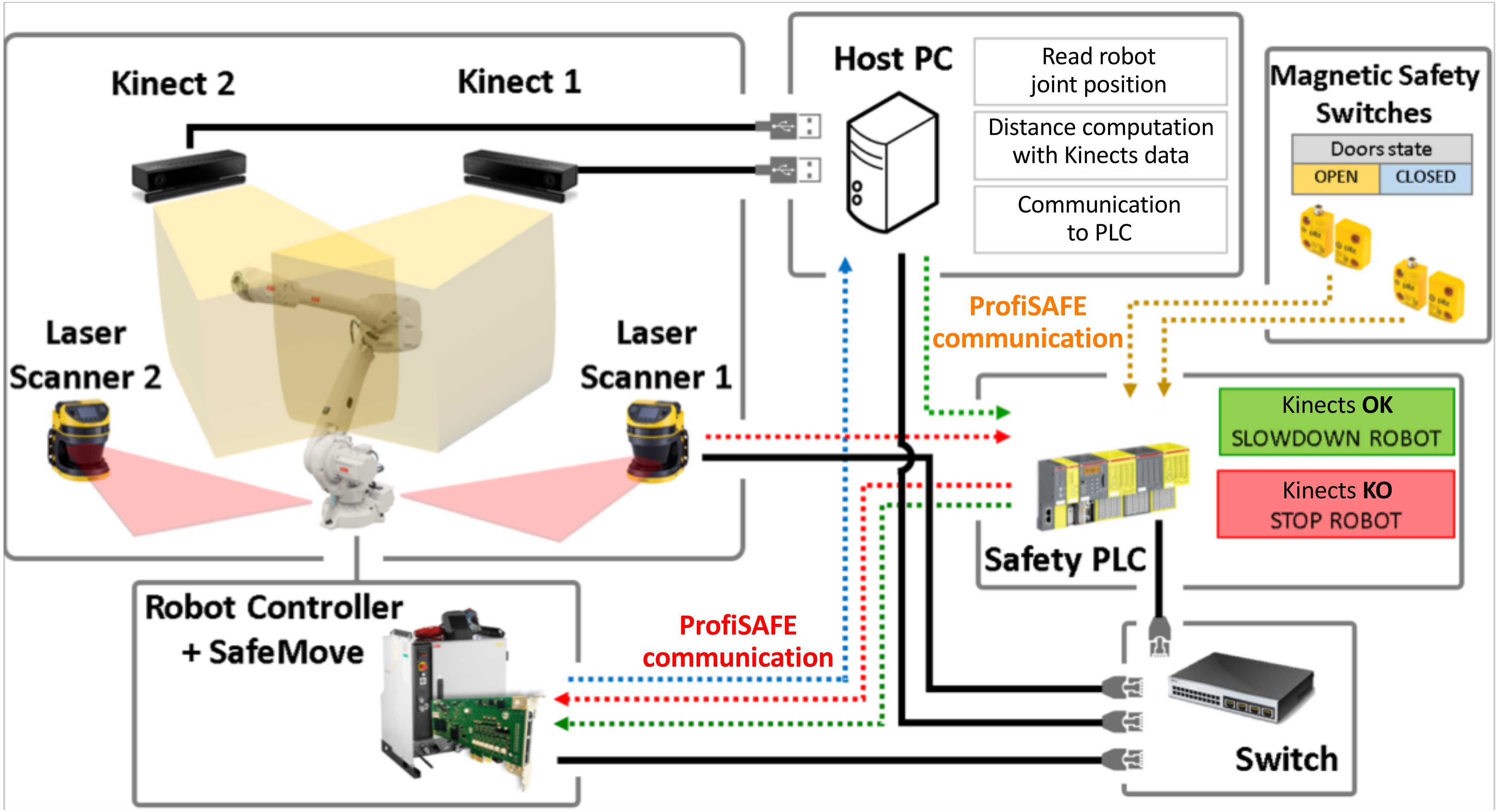

Force estimation for collaboration

Combining internal and external sensing

- Task
  - localize (in the least invasive way) points on robot surface where contacts occur
  - estimate exchanged **Cartesian** forces
  - control the robot to react to these forces according to a desired behavior
- Solution idea
  - use residual method to **detect** physical contact, **isolate** the colliding link, and **identify** the joint torques associated to the external contact force
  - use a depth sensor to **classify** the human parts in contact with the robot and **localize** the contact points on the robot structure (and the **contact Jacobian**)
  - **solve** a linear set of equations with the residuals, i.e., filtered estimates of joint torques resulting from contact forces/moments applied (anywhere) to the robot

$$\boldsymbol{r} \simeq \boldsymbol{\tau}_{ext} = \boldsymbol{J}_c^T(\boldsymbol{q})\boldsymbol{\Gamma}_c = \begin{pmatrix} \boldsymbol{J}_{L,c}^T(\boldsymbol{q}) & \boldsymbol{J}_{A,c}^T(\boldsymbol{q}) \end{pmatrix} \begin{pmatrix} \boldsymbol{F}_c \\ \boldsymbol{M}_c \end{pmatrix}$$

Force estimation

Some simplifying assumptions

- Dealing with contact forces
  - most intentional contacts with a single hand (or fingers) are not able to transfer non-negligible **torques**
  - to estimate reliably $\boldsymbol{\Gamma}_c$ we should have rank $\boldsymbol{J}_c = 6$ which is true only if the robot has $n \geq 6$ joints and contact occurs at a link with index greater or equal to 6

assume $\Big\downarrow$ $\boldsymbol{M}_c = \mathbf{0}$

only a **pure** Cartesian force is considered

  - dimension of the task related to the contact force is $m = 3$ and its **estimation** is

$$\boldsymbol{r} \simeq \boldsymbol{\tau}_{ext} = \boldsymbol{J}_{Lc}^T(\boldsymbol{q})\boldsymbol{F}_c \quad \Longrightarrow \quad \widehat{\boldsymbol{F}}_c = \left(\boldsymbol{J}_{Lc}^T(\boldsymbol{q})\right)^{\#} \boldsymbol{r}$$

  - the contact Jacobian can be evaluated once the contact point is detected by the external depth sensor closely monitoring the robot workspace

Force estimation

Some limitations of the residual method

- **multiple** simultaneous contacts can be considered (e.g., with **both** human hands)

$$\begin{pmatrix} \widehat{\boldsymbol{F}}_1 \\ \widehat{\boldsymbol{F}}_2 \end{pmatrix} = \begin{pmatrix} \boldsymbol{J}_{L1}^T(\boldsymbol{q}) & \boldsymbol{J}_{L2}^T(\boldsymbol{q}) \end{pmatrix}^{\#} \boldsymbol{r}$$

but with much less confidence in the resulting force estimates (detection is instead ok)

- **estimates** will be limited only to those components of $\boldsymbol{F}_c$ that can be detected by the residual

- all **forces** $\boldsymbol{F}_c \in \mathcal{N}(\boldsymbol{J}_c^T(\boldsymbol{q}))$ will never be recovered $\leftrightarrow$ they are absorbed by the robot structure

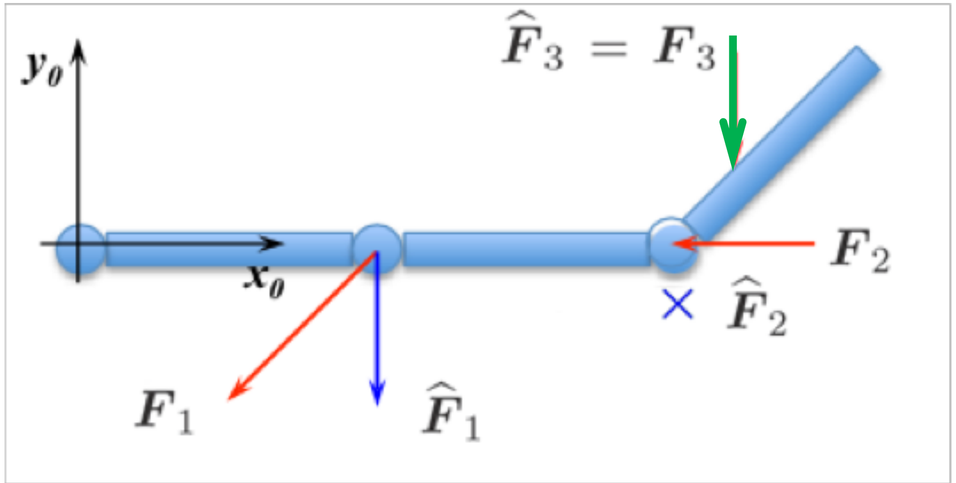

Validation of the virtual force sensor

Experiments with the KUKA LWR 4

- Evaluation of estimated contact force

$$\widehat{\boldsymbol{F}}_c = \left(\boldsymbol{J}_c^T(\boldsymbol{q})\right)^{\#} \boldsymbol{r}$$

  - estimation accuracy was tested using known masses in known positions
  - a single mass hung either on link 4 or on link 7, to emulate a **single** (point-wise) contact

			using $\boldsymbol{J}_{\boldsymbol{L}c}$		using $\boldsymbol{J}_c$	
Link #	Mass	F_z	$\widehat{F}_z$	Deviation	$\widehat{F}_z$	Deviation
4	1.93	-18.93	-18.75	0.95%	-4.46	76.43%
7	1.93	-18.93	-18.91	0.1%	-18.82	0.58%

  - a mass hung on link 7, and then a second on link 4 so as to emulate a **double** contact

Link #	Mass	F_z	$\widehat{F}_z$	Deviation
4	2.03	-19.91	-19.43	2.41%
7	1.93	-18.93	-19.04	0.58%

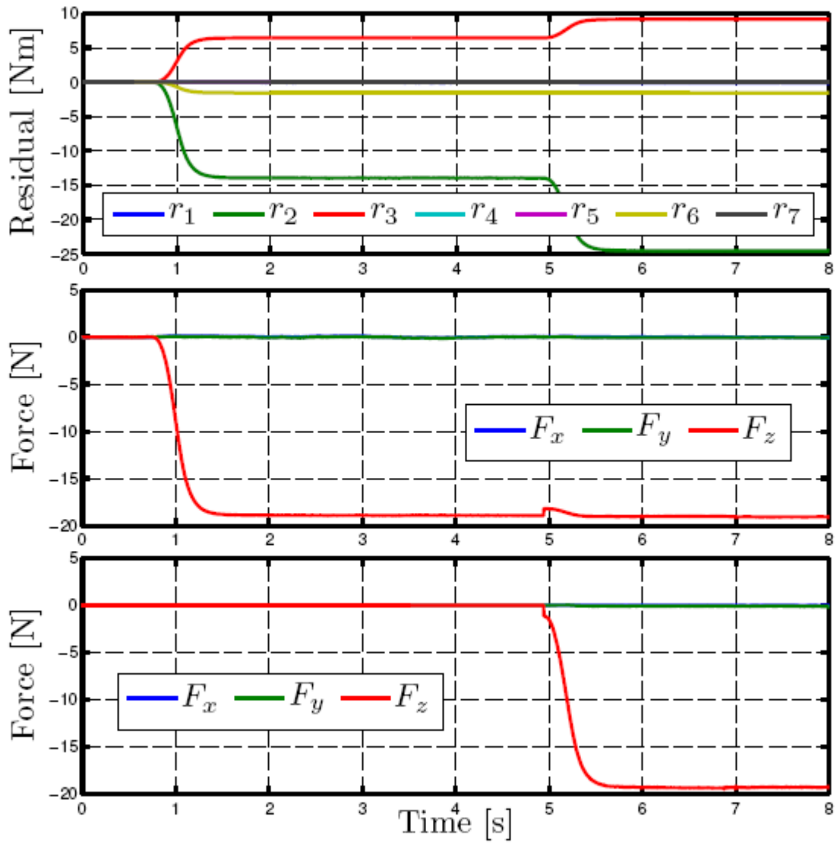

case of two masses

Contact force estimation

Used within an admittance control scheme (IROS 2014)

https://youtu.be/Yc5FoRGJsrc

Estimation of the contact force

Sometimes, even without external sensing

- if contact is sufficiently "down" the kinematic chain (**≥ 6 residuals** are available), the estimation of pure contact forces does not need any external information ...

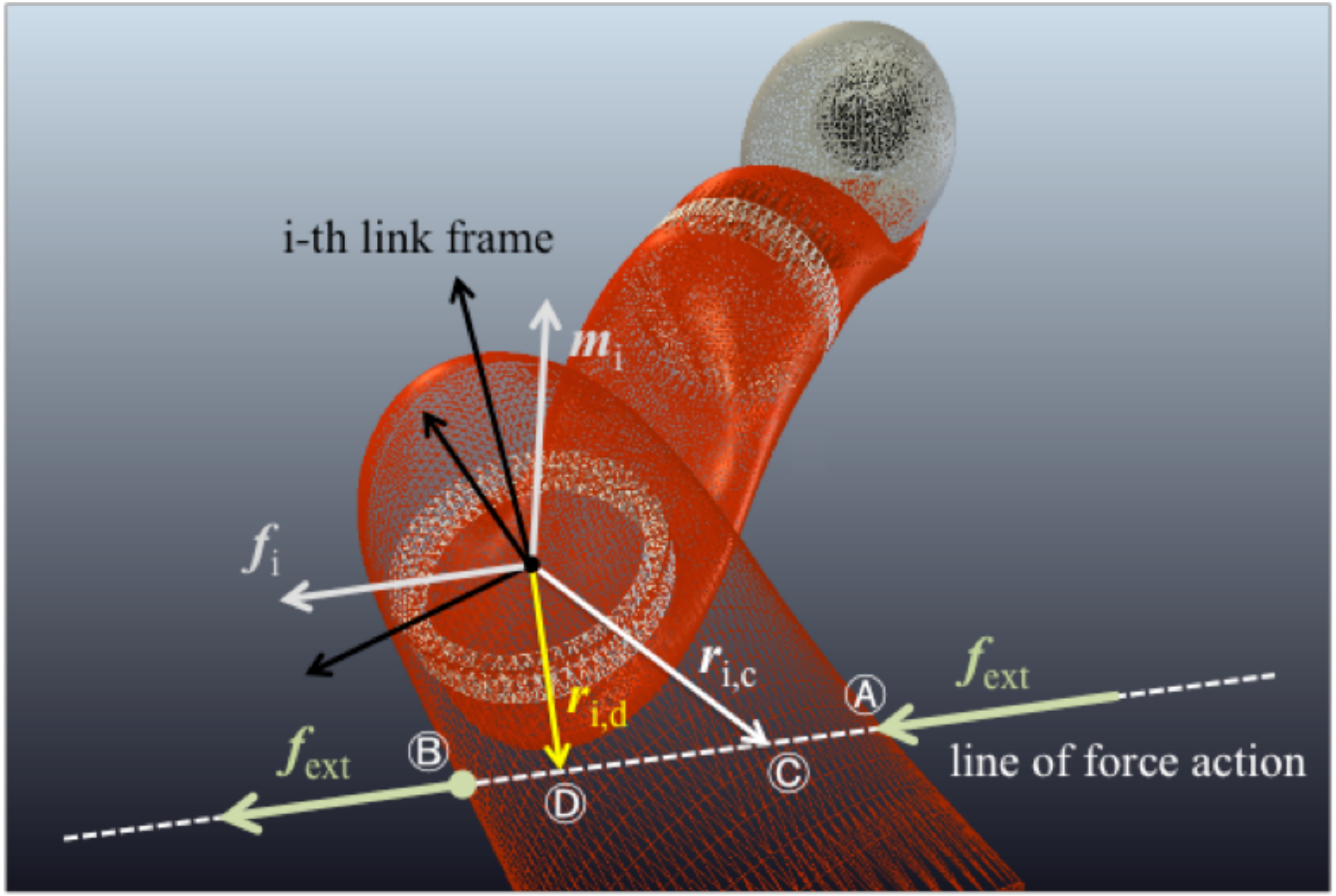

Collision or collaboration?

Distinguishing hard/accidental collisions and soft/intentional contacts

- using suitable low and high bandwidths for the residuals (first-order stable filters)

$$\dot{\boldsymbol{r}} = -\boldsymbol{K}_I \boldsymbol{r} + \boldsymbol{K}_I \boldsymbol{\tau}_K$$

- a threshold is added to prevent false collision detection during robot motion

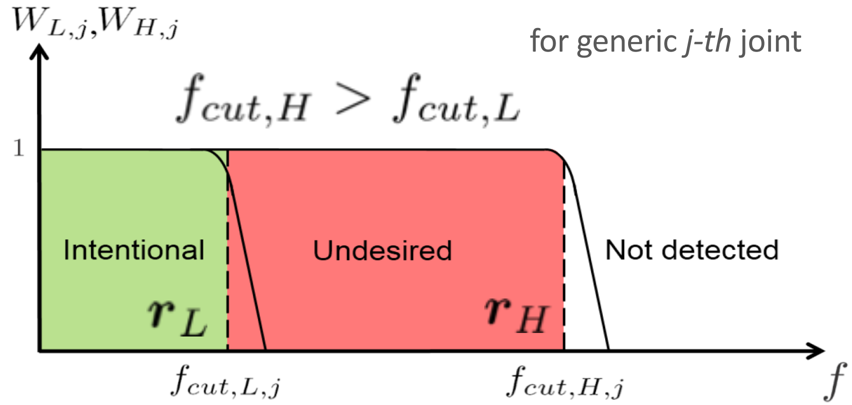

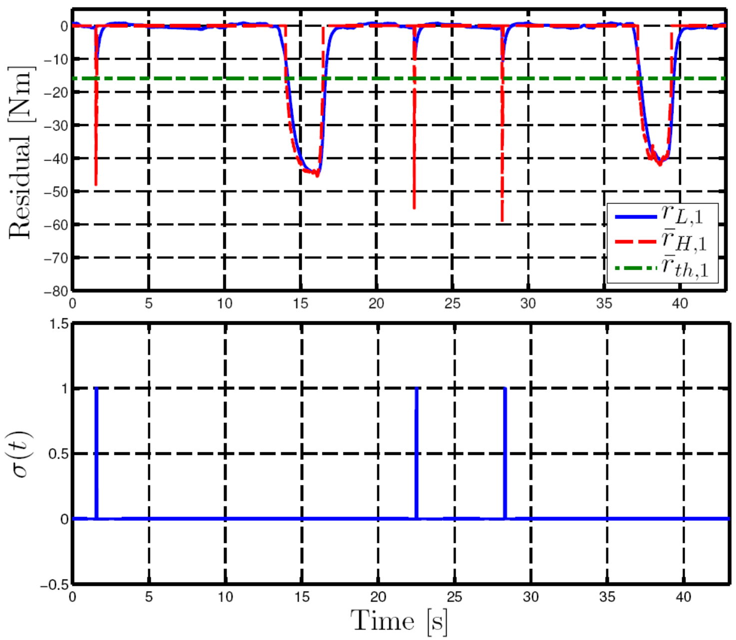

Collaboration control

How to use the estimate on an external contact force for control (e.g., on a Kuka LWR)

- shaping the robot dynamic behavior in specific collaborative tasks
  - joint carrying of a load, holding a part in place, whole arm **force** manipulation, ...
  - robot motion controlled by
    - an **admittance** control law (in **velocity FRI** mode)
    - an **impedance** or **force** control laws (needs **torque FRI** mode)

  all implemented **at contact level**

- e.g., admittance control law using the estimated contact force
  - the scheme is realized at the single (or first) contact point
  - desired **velocity** of contact point taken proportional to (**estimated**) contact force

$$\dot{\boldsymbol{p}}_c = \boldsymbol{K}_a \boldsymbol{F}_a, \qquad \boldsymbol{K}_a = k_a \boldsymbol{I} > 0$$

$$\boldsymbol{F}_a = \widehat{\boldsymbol{F}}_c + \boldsymbol{K}_p(\boldsymbol{p}_d - \boldsymbol{p}_c), \qquad \boldsymbol{K}_p = k_p \boldsymbol{I} > 0$$

initial contact point position when interaction begins

Virtual force sensing for contact force regulation

Human-robot collaboration in torque control mode (ICRA 2015)

- contact force estimation & control (anywhere/anytime)

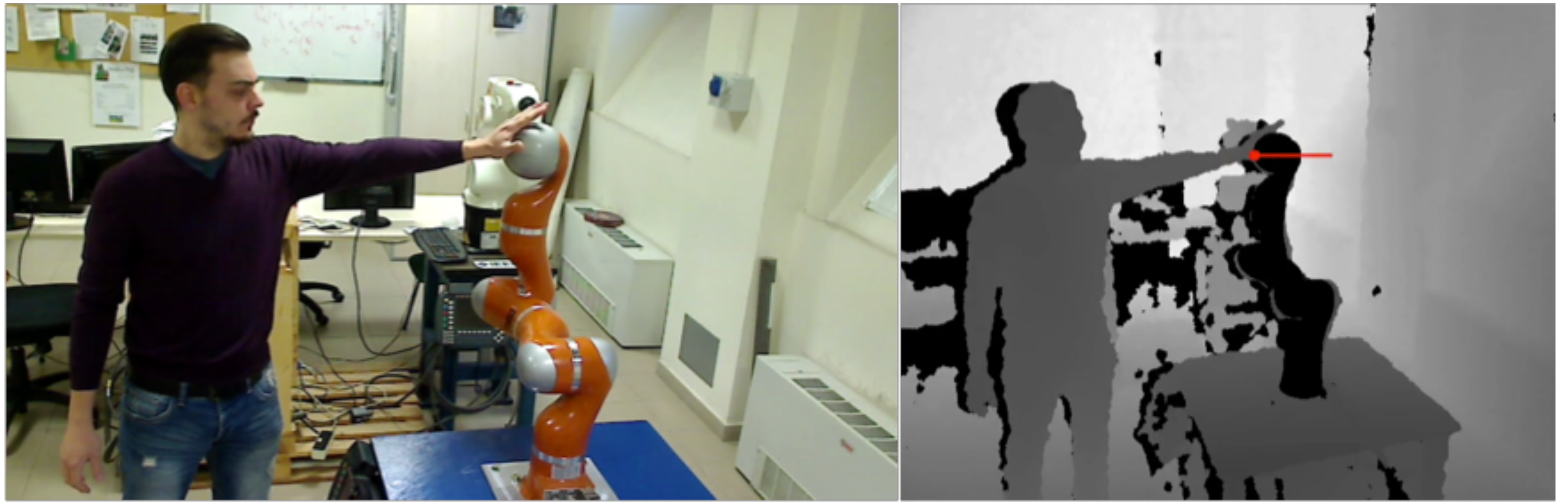

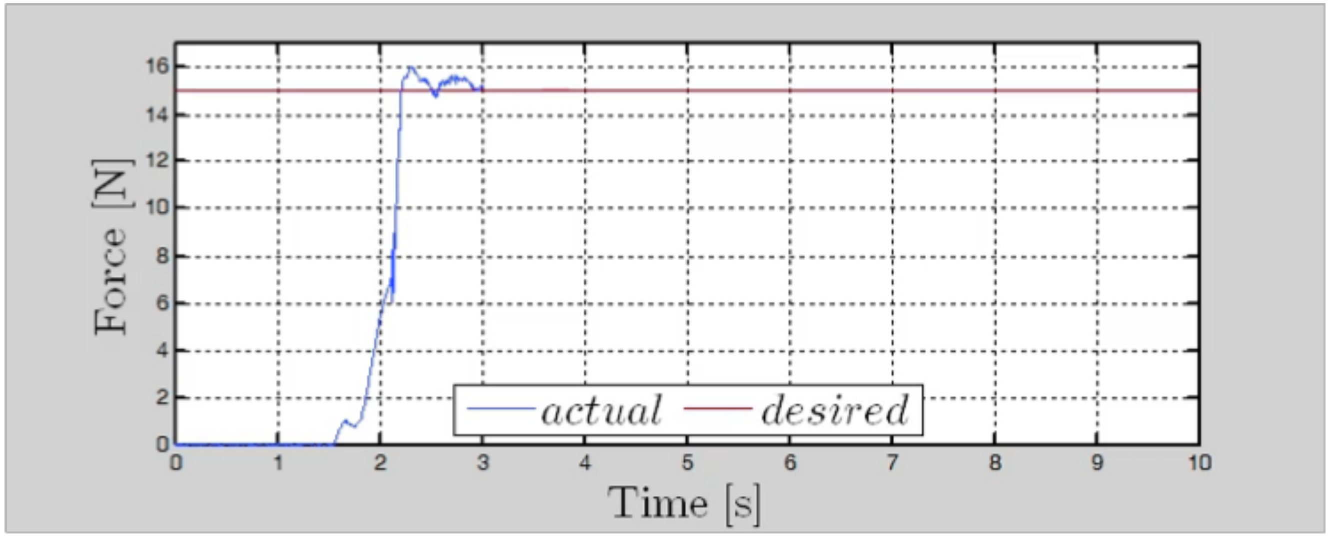

see also ICRA 2015 trailer (at 3’26’’): https://youtu.be/glNHq7MpCG8 (italian); https://youtu.be/OM_1F33fcWk (english)

Impedance-based control of interaction

Reaction to contact forces by generalized impedance —at **different** levels

consider a fully rigid robot

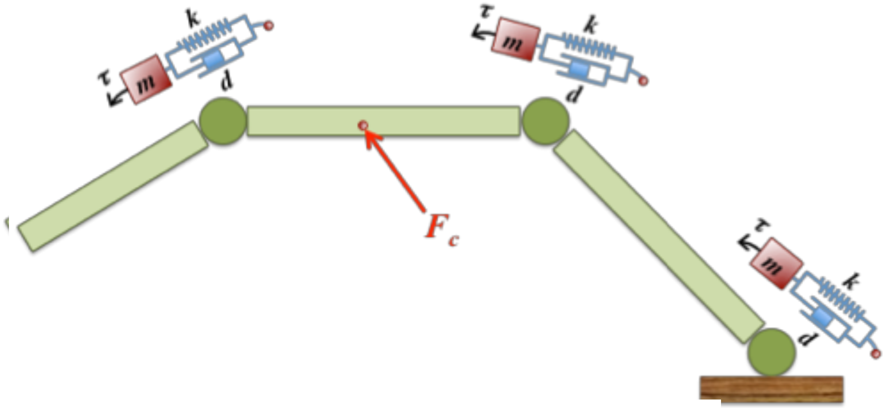

Joint impedance
needs joint torque sensors

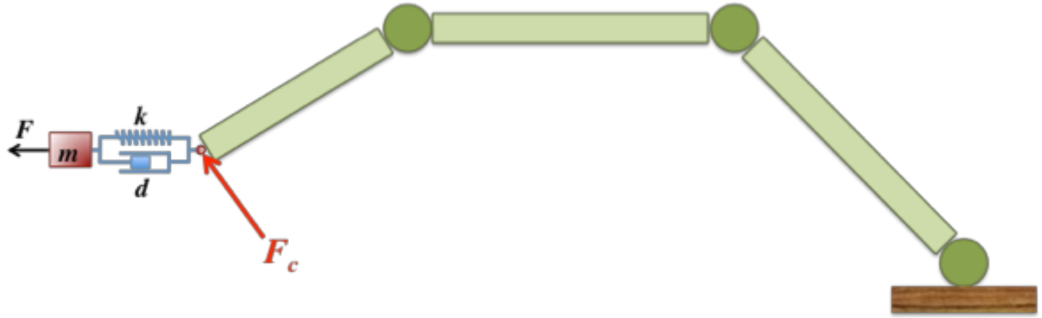

Cartesian impedance
needs F/T sensor

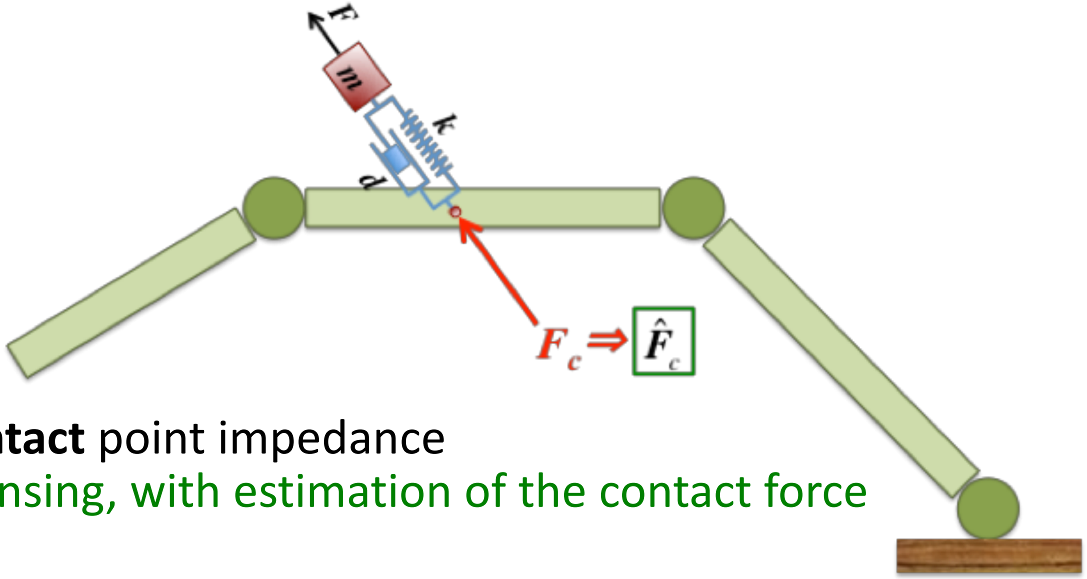

Contact point impedance
without force/torque sensing, with estimation of the contact force

Control of generalized impedance

HR collaboration at the contact level (ICRA 2015)

https://youtu.be/NHn2cwSyCCo for these and the next two videos

natural (unchanged) robot inertia at the contact

$$M_d = \left(J_c M^{-1} J_c^T\right)^{-1}$$

assigned robot inertia at the contact
with different desired masses along X, Y, Z

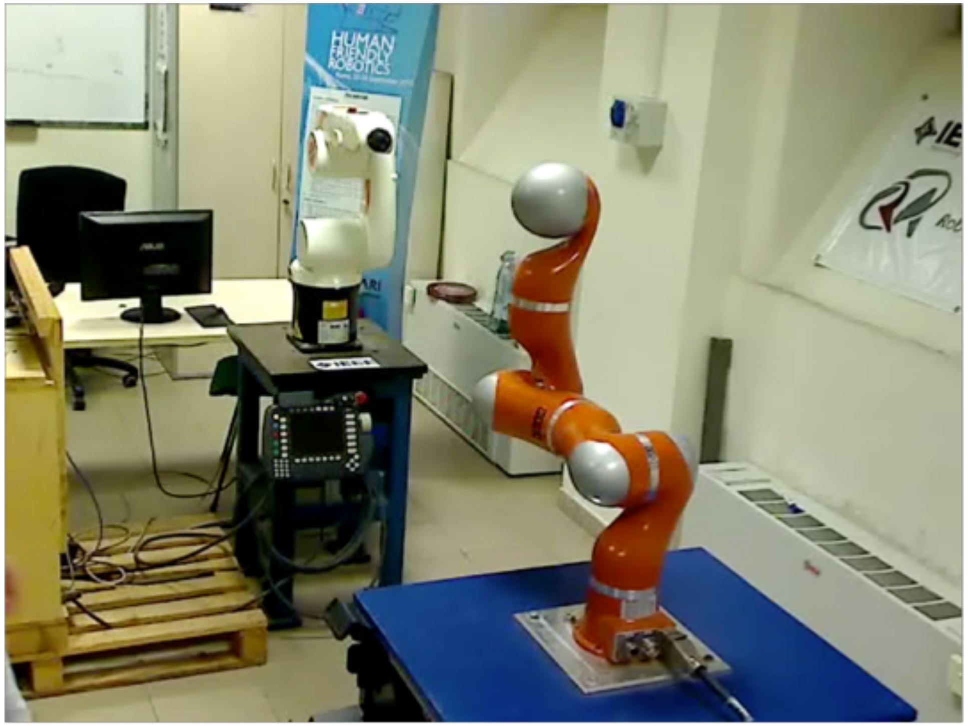

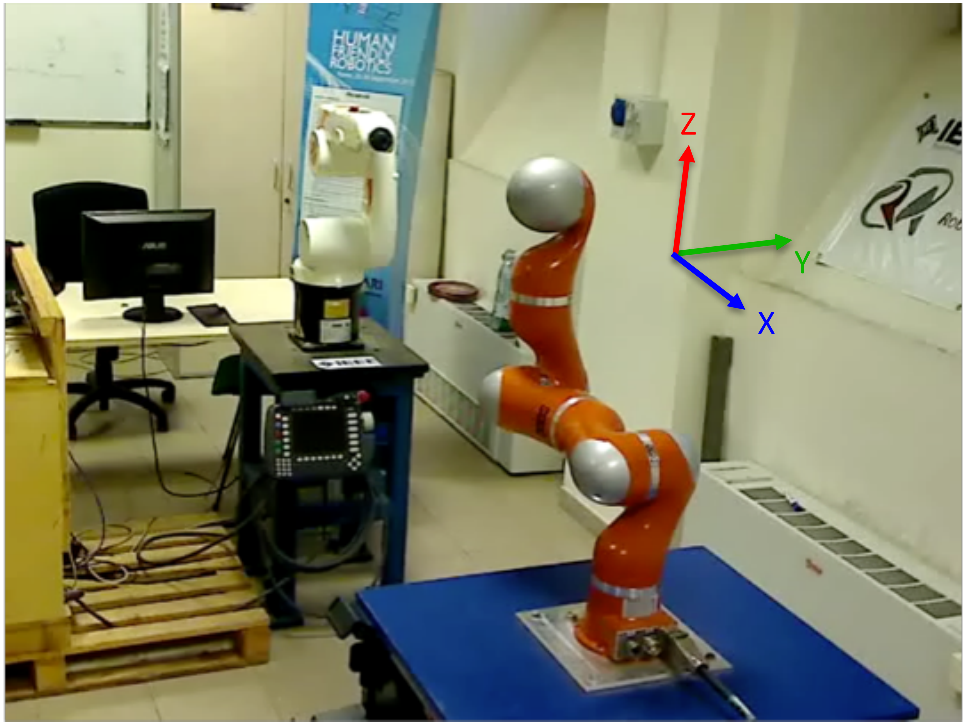

contact force **estimates** are used here **only** to detect and localize contact in order to start a collaboration phase

contact force **estimates** used **explicitly** in control law to modify robot inertia at the contact (M_{dX} = 20, M_{dY} = 3, M_{dZ} = 10 [kg])

Control of generalized contact force

Direct force scheme

- explicit **regulation** of the **contact force** to a desired value, by imposing

$$\boldsymbol{M}_d \ddot{\boldsymbol{x}}_c + \boldsymbol{K}_d \dot{\boldsymbol{x}}_c = \boldsymbol{K}_f (\boldsymbol{F}_d - \widehat{\boldsymbol{F}}_c) = \boldsymbol{K}_f \boldsymbol{e}_f$$

- a force control law needs always a measure (here, an **estimate**) of contact force
- **task-compatibility**: human-robot contact direction vs. desired contact force vector

$F_{d,x} = 0, \quad F_{d,y} = 15N, \quad F_{d,z} = 0$

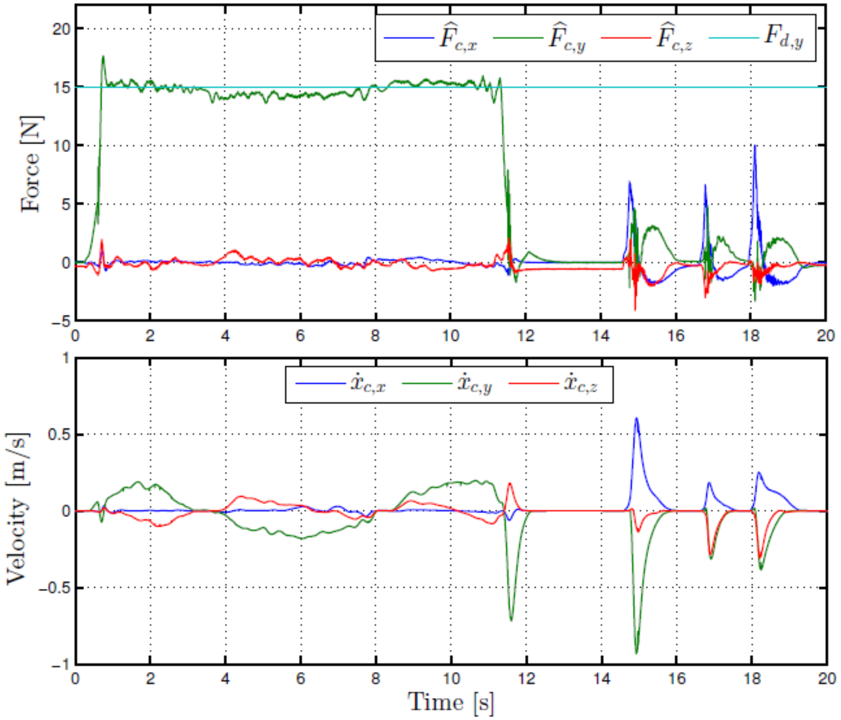

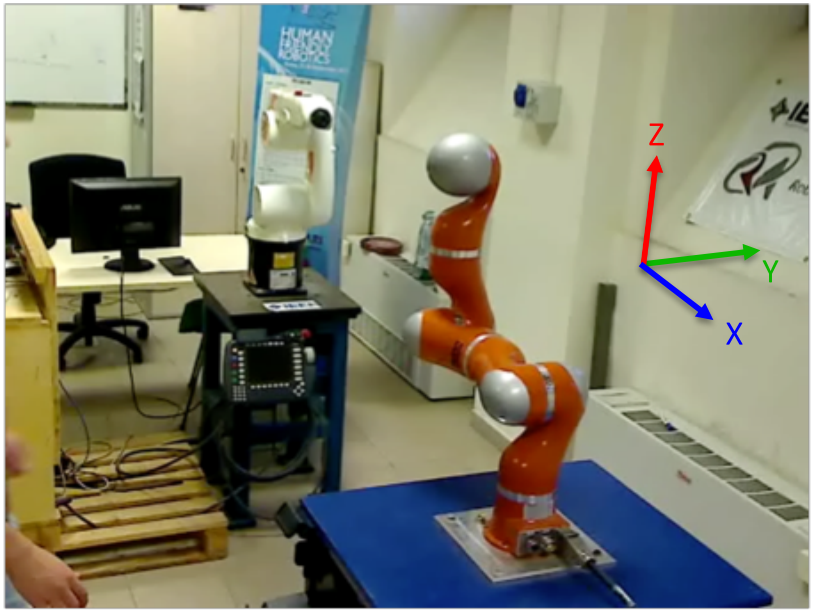

drift effects in poor control of contact force

- only the **norm** of the desired contact force is controlled along the instantaneous **direction** of the estimated contact force

$$F_{d,x} = 15 \frac{\widehat{F}_{c,x}}{\|\widehat{\boldsymbol{F}}_c\|}, \quad F_{d,y} = 15 \frac{\widehat{F}_{c,y}}{\|\widehat{\boldsymbol{F}}_c\|}, \quad F_{d,z} = 15 \frac{\widehat{F}_{c,z}}{\|\widehat{\boldsymbol{F}}_c\|} \quad \Leftrightarrow \quad \|F_d\| = 15 \ [\mathrm{N}]$$

- force control law is able to regulate exactly contact forces under static conditions

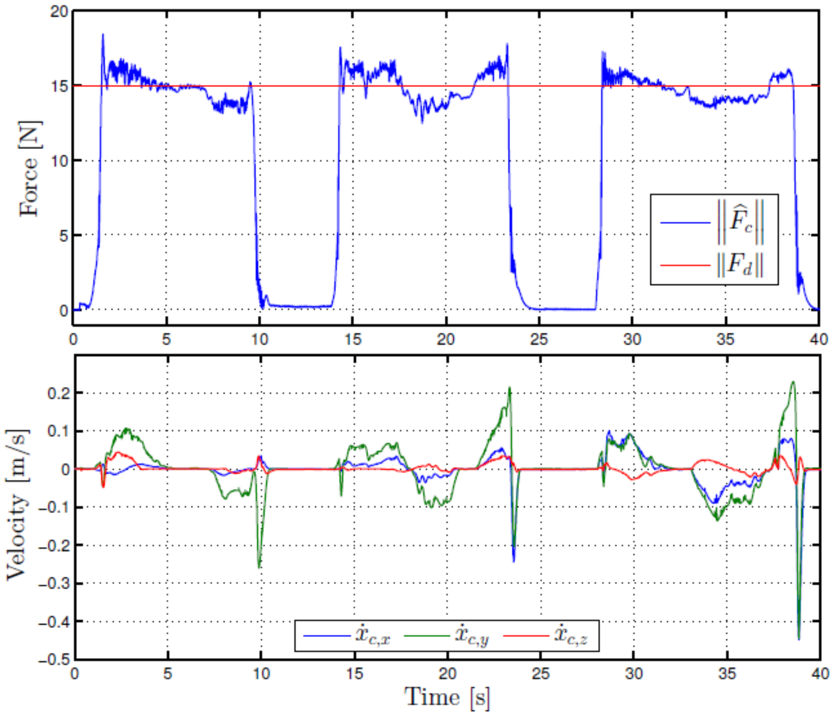

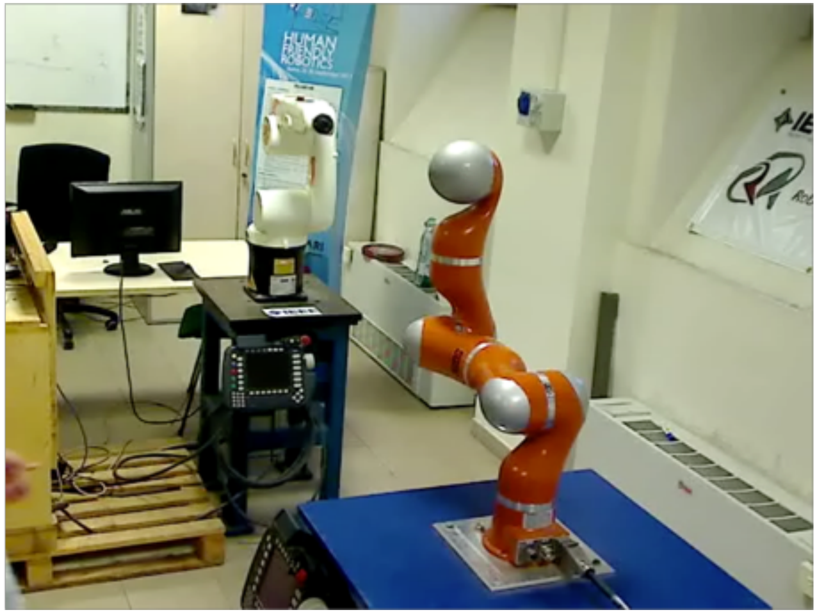

task-compatible control of contact force

Collaboration control

Hybrid force/velocity control scheme (ICRA 2016)

- it allows to control both contact force and motion in **two** mutually independent sub-spaces
- extends at the contact level a hybrid force/velocity control law, with the orientation of **contact task frame** being determined instantaneously
- task frame obtained by a rotation matrix $\boldsymbol{R}_t$ such that $\boldsymbol{z}_t$ is aligned with the contact force $\boldsymbol{F}_c$

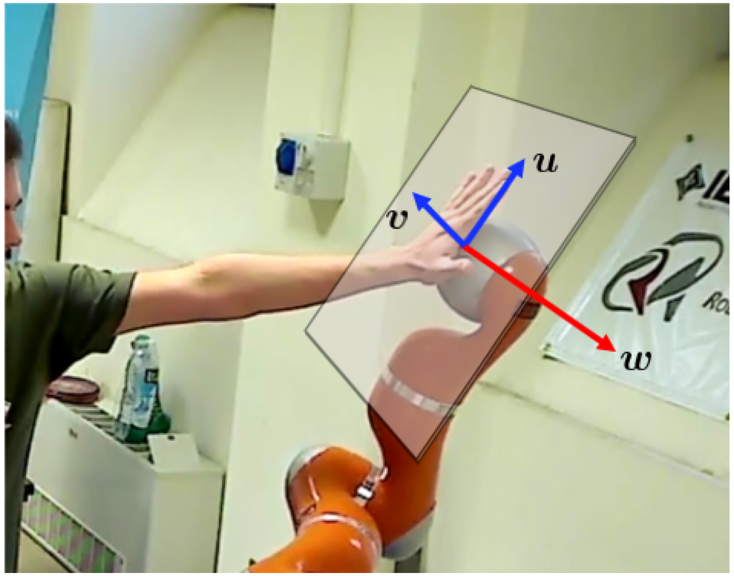

$$\boldsymbol{R}_t = \left[\begin{array}{ccc} \boldsymbol{u} & \boldsymbol{v} & \boldsymbol{w} \end{array}\right] = \left[\begin{array}{ccc} \boldsymbol{u} & \boldsymbol{v} & \dfrac{\widehat{\boldsymbol{F}}_c}{\|\widehat{\boldsymbol{F}}_c\|}, \end{array}\right]$$

- the auxiliary command is given by

$$\boldsymbol{a} = \boldsymbol{J}_c^{\#} \boldsymbol{M}_d^{-1} (\boldsymbol{R}_t \boldsymbol{a}_c + \boldsymbol{M}_d (\dot{\boldsymbol{R}}_t {}^t\dot{\boldsymbol{x}}_c - \dot{\boldsymbol{J}}_c \dot{\boldsymbol{q}})) + \boldsymbol{P}_c \ddot{\boldsymbol{q}}_0$$

- a complete decoupling between force control and velocity control can be achieved choosing the new auxiliary control input as

$$\boldsymbol{a}_c = \boldsymbol{S}_f^c \, \ddot{y}_f + \boldsymbol{S}_\nu^c \, \dot{\boldsymbol{\nu}}$$

Collaboration control

Hybrid force/velocity control scheme

- consider a force regulation task along the instantaneous direction of the applied external force and a motion control task in the orthogonal plane
- *selection matrices* can be chosen as

$$\boldsymbol{S}_f^c = \begin{bmatrix} 0 \\ 0 \\ 1 \end{bmatrix} \qquad \boldsymbol{S}_\nu^c = \begin{bmatrix} 1 & 0 \\ 0 & 1 \\ 0 & 0 \end{bmatrix}$$

- regulation of the contact force to desired constant value $F_d > 0$ is obtained choosing

$$\ddot{y}_f = k_f \left(F_d - \|\widehat{\boldsymbol{F}}_c\| \right) - k_{df}\dot{y}_f$$

- the desired velocity can be achieved using the control law

$$\dot{\boldsymbol{\nu}} = \dot{\boldsymbol{\nu}}_d + \boldsymbol{K}_d (\boldsymbol{\nu}_d - \boldsymbol{\nu}) + \boldsymbol{K}_i \int_0^t (\boldsymbol{\nu}_d - \boldsymbol{\nu}) \, \boldsymbol{d}s,$$

- final control input becomes

$$\boldsymbol{a} = \boldsymbol{J}_c^{\#} \boldsymbol{M}_d^{-1} \Big[\boldsymbol{R}_t \boldsymbol{S}_f^c (k_f e_f - k_{df}\dot{y}_f) + \boldsymbol{R}_t \boldsymbol{S}_\nu^c (\dot{\boldsymbol{\nu}}_d + \boldsymbol{K}_d \dot{\boldsymbol{e}}_{\boldsymbol{\nu}} + \boldsymbol{K}_i \boldsymbol{e}_{\boldsymbol{\nu}})$$
$$+ \boldsymbol{M}_d \dot{\boldsymbol{R}}_t {}^c\dot{\boldsymbol{x}} - \boldsymbol{M}_d \dot{\boldsymbol{J}}_c \dot{\boldsymbol{q}} \Big] + \boldsymbol{P}_c \ddot{\boldsymbol{q}}_0,$$

https://youtu.be/tIhEK5f00QU for this and next video

- desired contact force along Y direction regulated to $\boldsymbol{F}_d = 15[N]$
- constant desired velocity to perform a line in the vertical XZ plane

$$\boldsymbol{\nu}_d = \begin{bmatrix} 0.015 \\ 0.03 \end{bmatrix} \qquad \dot{\boldsymbol{\nu}}_d = \begin{bmatrix} 0 \\ 0 \end{bmatrix}$$

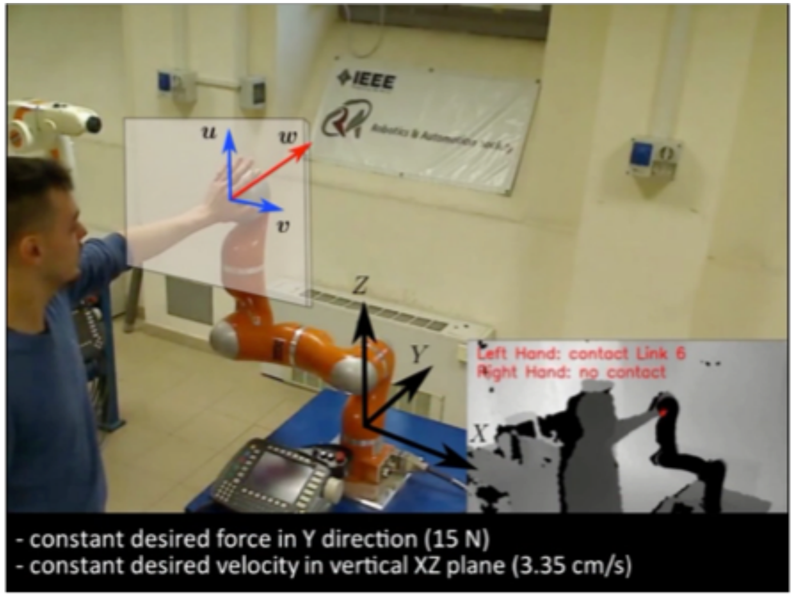

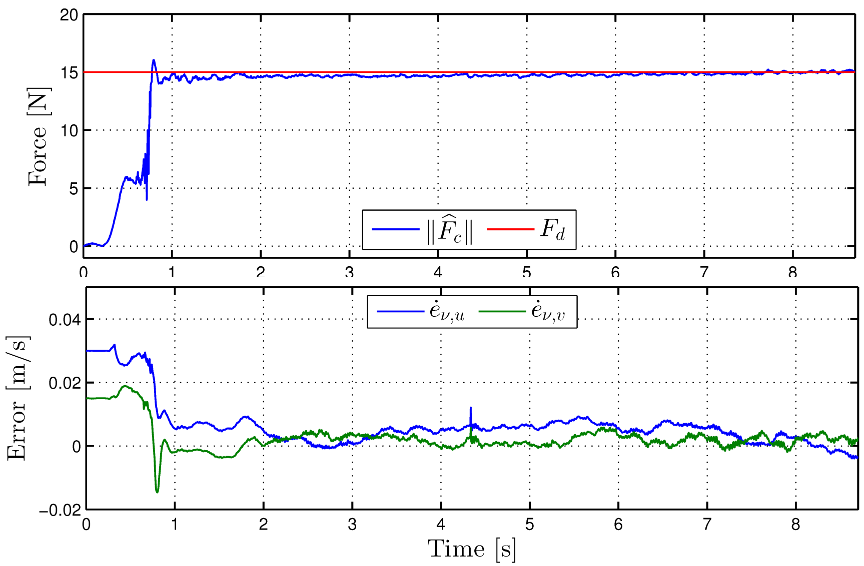

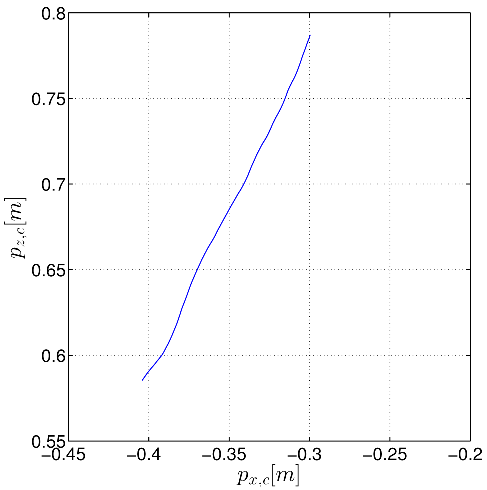

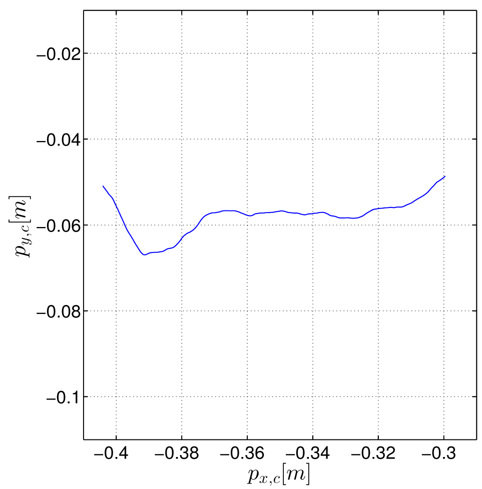

Collaboration control

Hybrid force/velocity control at contact level (IROS 2016)

- desired contact force along the X direction regulated to $\boldsymbol{F}_d = 15[N]$
- desired velocity/acceleration to perform a circle in the vertical YZ plane

$$\boldsymbol{\nu}_d = \begin{bmatrix} \omega\rho \sin\omega t \\ \omega\rho \cos\omega t \end{bmatrix} \qquad \dot{\boldsymbol{\nu}}_d = \begin{bmatrix} \omega^2\rho \cos\omega t \\ -\omega^2\rho \sin\omega t \end{bmatrix}$$

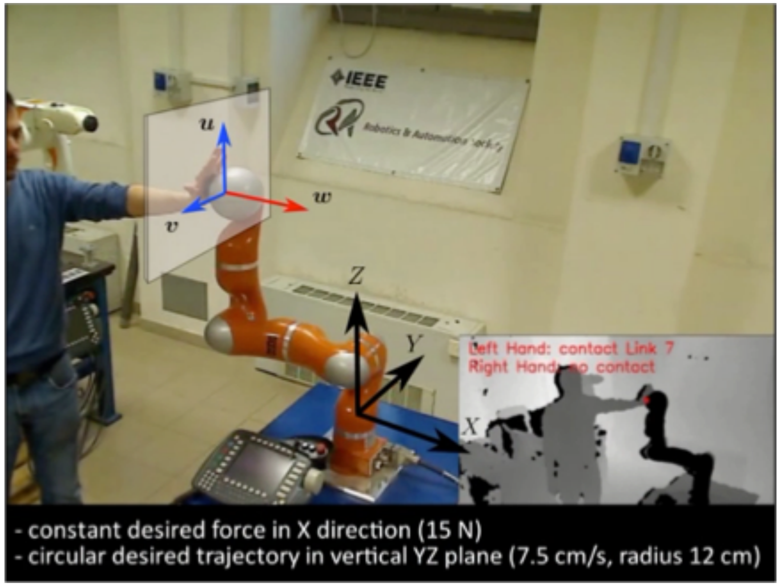

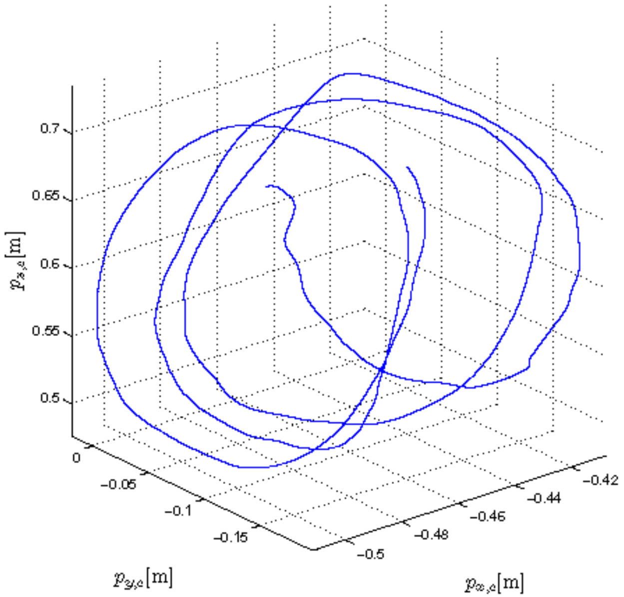

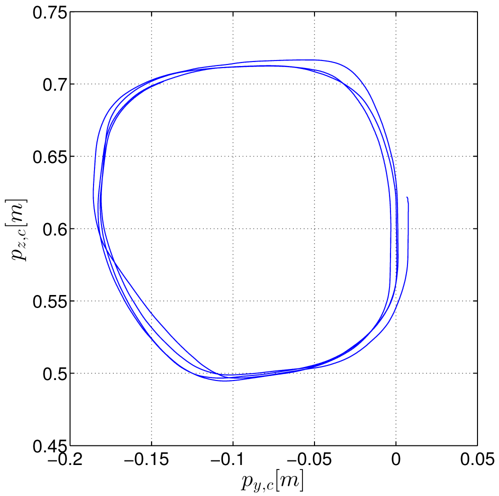

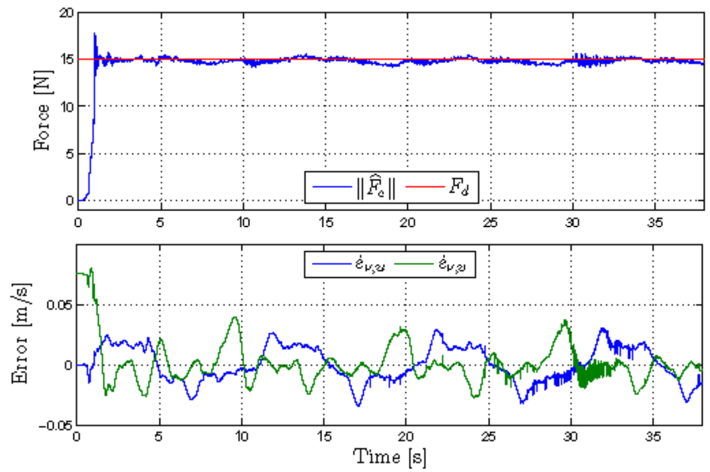

Scenario for HRC in manual polishing

EU SYMPLEXITY project: preparing a metallic part for a laser polishing machine

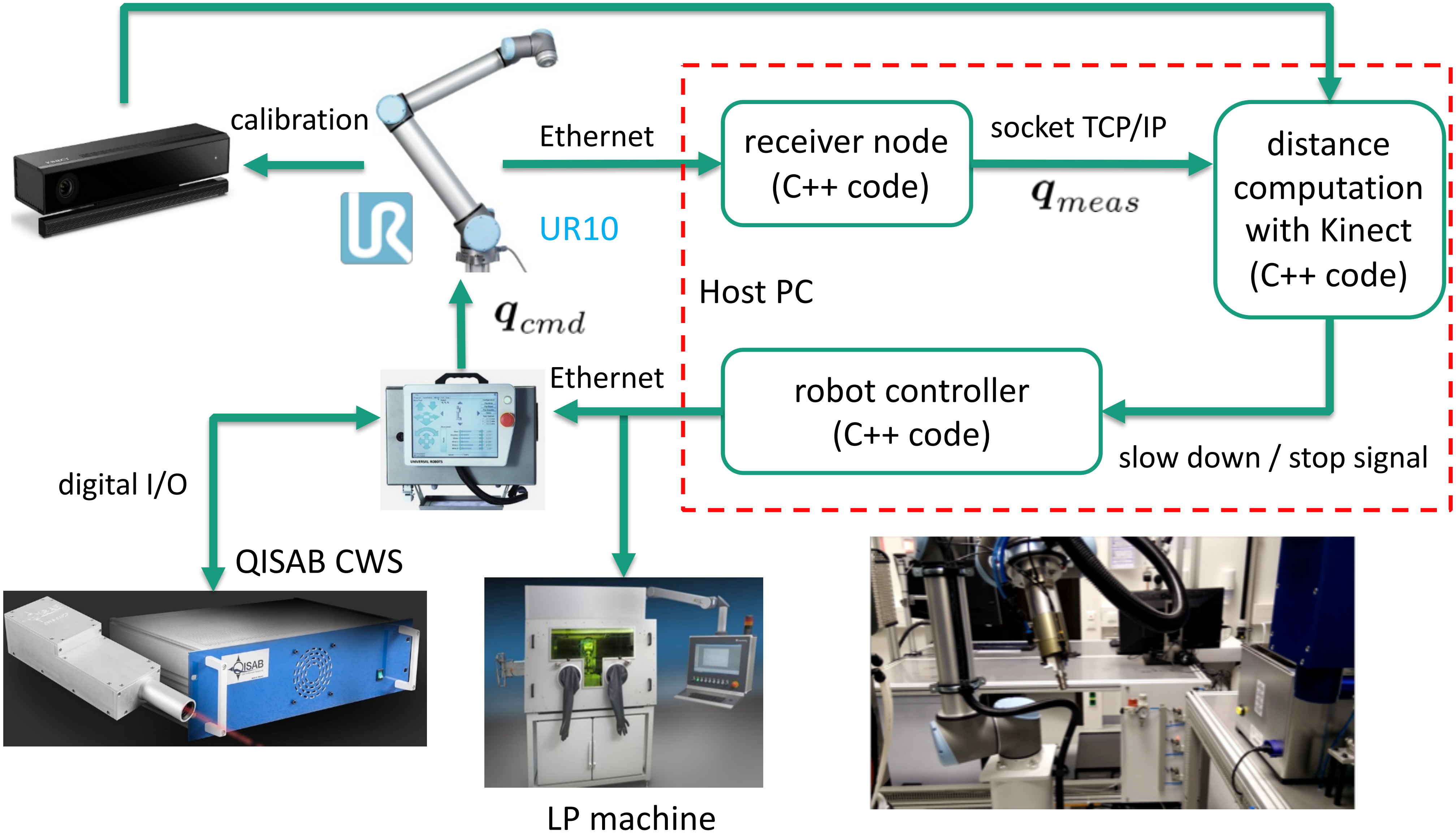

Scenario for HRC in manual polishing

Distinguishing different contact forces

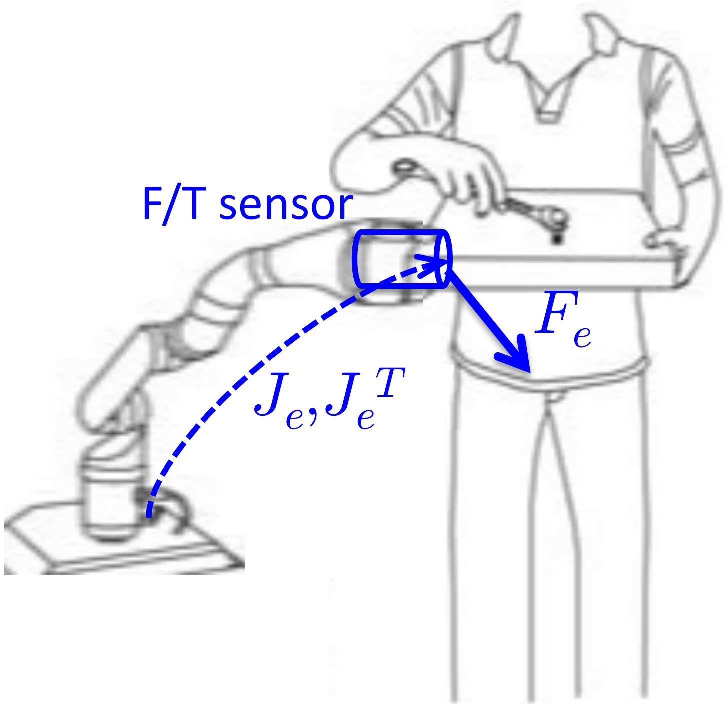

Force/Torque (F/T) sensor at wrist
- manual polishing force is **measured**
- end-effector Jacobian is **known**

contact force at unknown location
- **not** measurable by the F/T sensor
- possibly applied by the human **while** manipulating the work piece held by robot
- contact Jacobian is **not** known

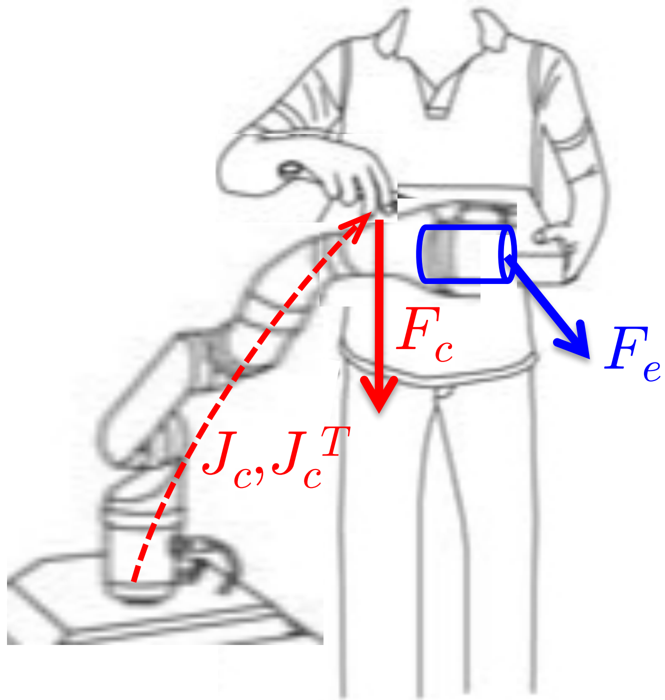

Handling multiple contacts

Dynamic model and residual computation

- robot **dynamic model** takes the form

$$M(q)\ddot{q} + C(q,\dot{q})\dot{q} + g(q) = \tau + J_e^T(q)F_e + J_c^T(q)F_c$$

- joint torques resulting from different contacts

(measured) at the end-effector level

$$\tau_e = J_e^T(q)F_e$$

at a generic point along the structure

$$\tau_c = J_c^T(q)F_c$$

- monitor the robot generalized momentum $p = M(q)\dot{q}$

- (model-based) **residual vector** signal to detect and isolate the generic contacts

$$r(t) = K_i\left(p - \int_0^t \left(C^T(q,\dot{q})\dot{q} - g(q) + \tau + J_e^T(q)F_e - r\right) ds\right)$$

$$\boxed{K_i \to \infty \text{ (sufficiently large)} \quad \Rightarrow \quad r \simeq \tau_c}$$

Control strategy during manual polishing

Human and robot are physically collaborating

- when there is no extra contact along the structure, **position and orientation** of the end-effector are both held **fixed** by a **stiff** **kinematic control law**

$$\dot{q} = \underbrace{J_e^{\#} K_e}_{\text{as large as possible}} \begin{pmatrix} v_r \\ \omega_r \end{pmatrix} = J_e^{\#} K_e \begin{pmatrix} I & 0 \\ 0 & T(\phi) \end{pmatrix} \begin{pmatrix} p_d - p \\ \phi_d - \phi \end{pmatrix}$$

as large as possible

constant values

- the controller counterbalances all forces/torques applied by the operator **during manual polishing**
- when the human intentionally pushes on the robot body, control of the end-effector **orientation** is **relaxed**

3×6 for UR10

$$J_e(q) = \begin{pmatrix} J_p(q) \\ J_o(q) \end{pmatrix}$$

residual-based reaction to extra contacts

$$\boxed{\dot{q} = J_p^{\#} K_p (p_d - p) + \overbrace{\left(I - J_p^{\#} J_p\right) K_r r}}$$

- human can reconfigure the arm, thus **reorient the work piece** held by the robot

HRC phase with UR10

Experimental results (Mechatronics 2018)

https://youtu.be/slwUiRT_IJQ

no F/T sensor, switching to FreeDrive mode

https://youtu.be/bjZbmlAclYk

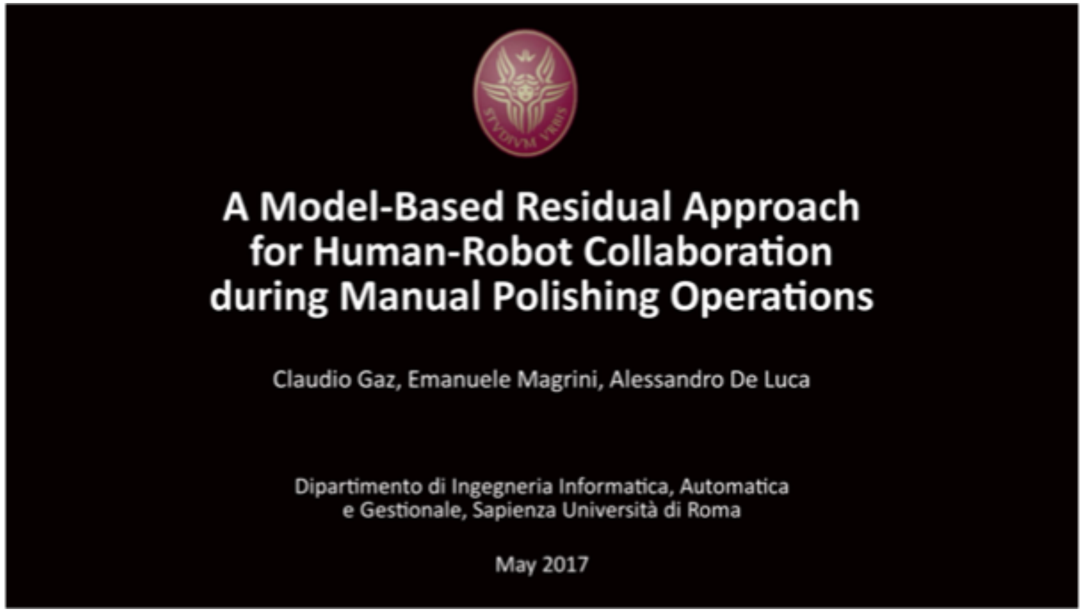

with F/T sensor, using residual method

⇓

(Special issue on HRC
in industrial applications)

part to be
polished

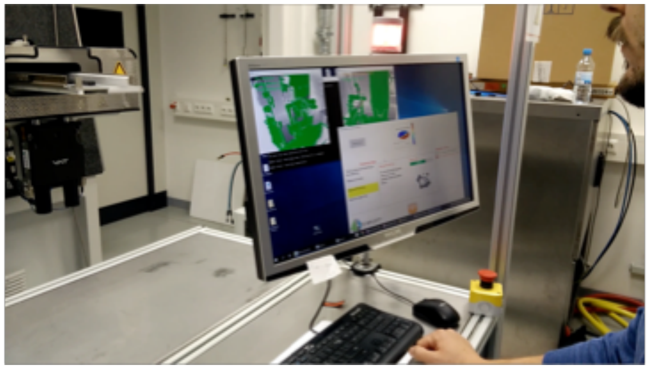

for a similar video on the KUKA LWR, see
https://youtu.be/TZ6nPqLPDxI

HRC phase with UR10

Experimental results

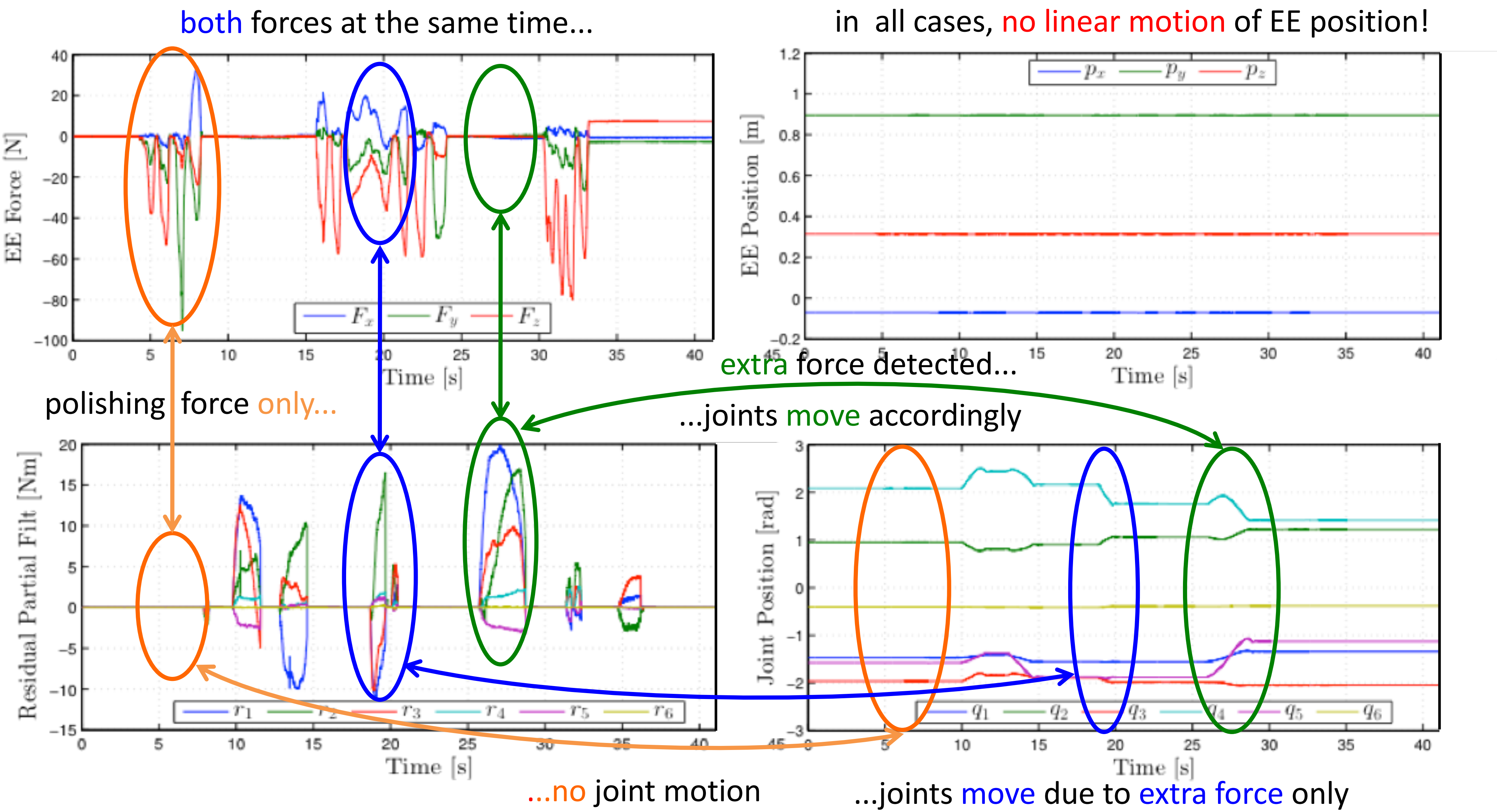

Use of kinematic redundancy in pHRI

Robot reaction to collisions, in parallel with execution of original task

- collision detection $\Rightarrow$ robot reacts so as to preserve as much as possible (if at all possible) the execution of a planned task trajectory, e.g., for the end-effector

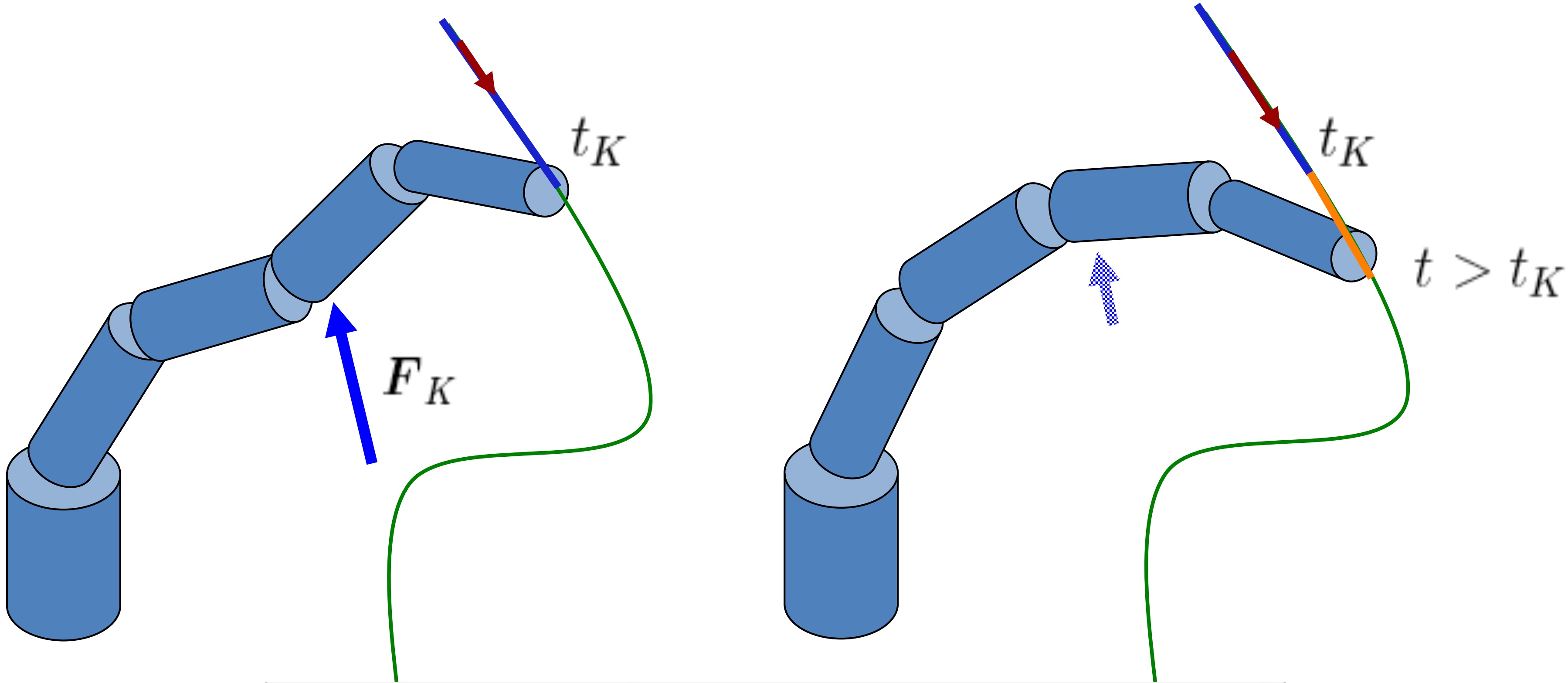

$$\boxed{\tau} = M(q)G(q)\left[\ddot{x} - \dot{J}(q)\dot{q} + J(q)M^{-1}(q)n(q,\dot{q})\right] + M(q)(I - G(q)J(q))M^{-1}(q)\tau_0$$

Selective reaction to estimated contact force

Robot control strategy (IROS 2017)

- the control scheme **exploits robot redundancy** in order to follow a Cartesian trajectory, despite the possible occurrence of accidental collisions on the robot body
- execution of the original end-effector motion task is preserved while reacting to a detected contact, with the **estimated contact force** above a threshold F_{relax} but **not too large**
- using null-space motion, the robot tries to **eliminate, reduce** or **keep low** the contact force
- if the contact force exceeds a threshold F_{abort} , the robot abandons the original task and reacts by imposing **admittance control at the contact**

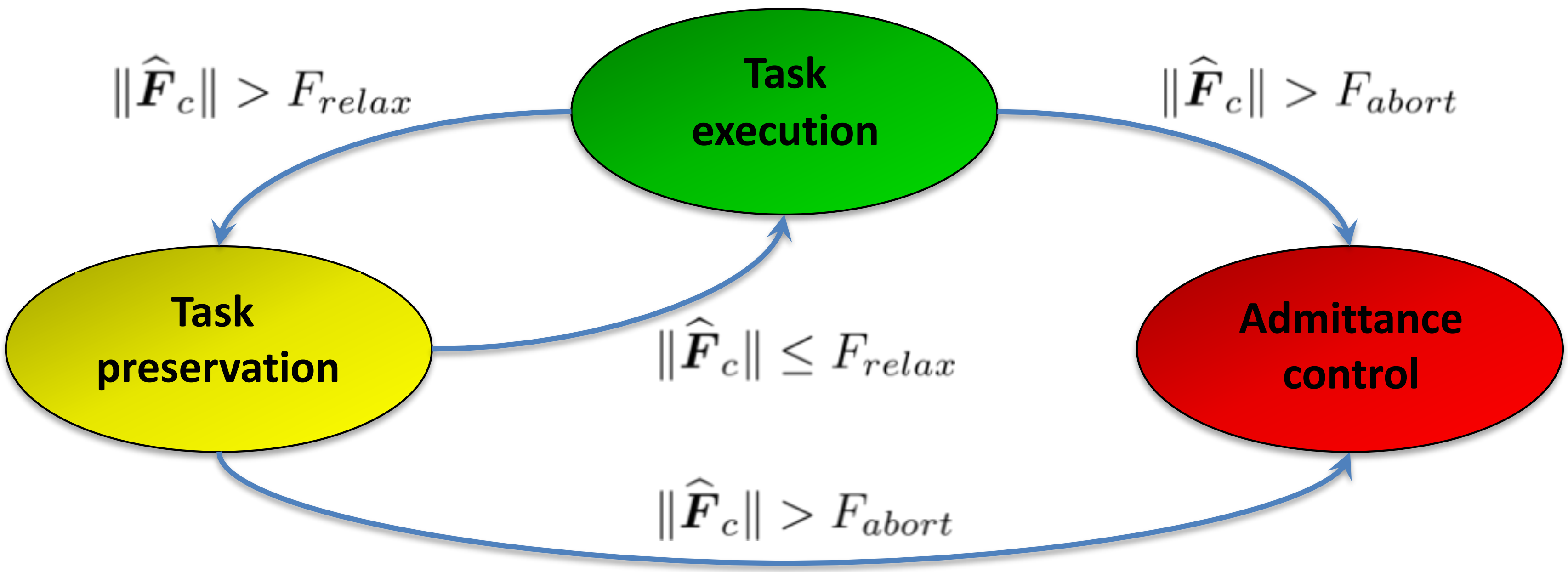

Use of kinematic redundancy

Robot reaction to collisions, in parallel with execution of original task (IROS 2017)

https://youtu.be/q4PZKE-kgc0

idle ⇔ relax ⇔ abort

pHRI experiments

Analysis of results

...and **no** task perturbation

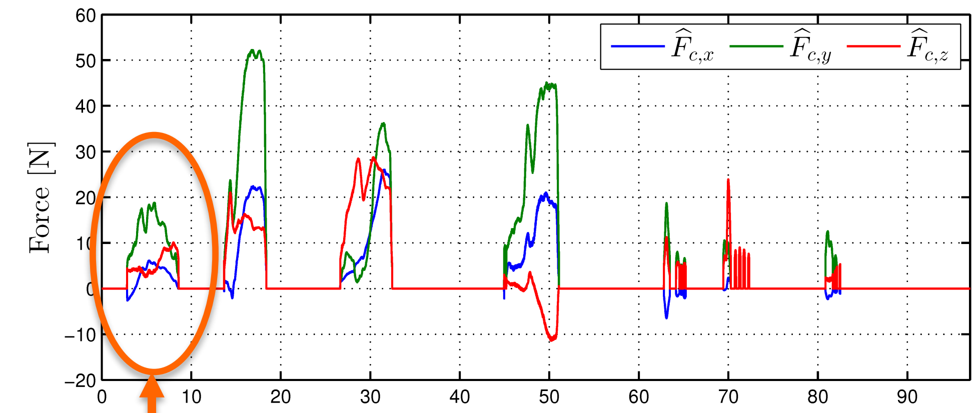

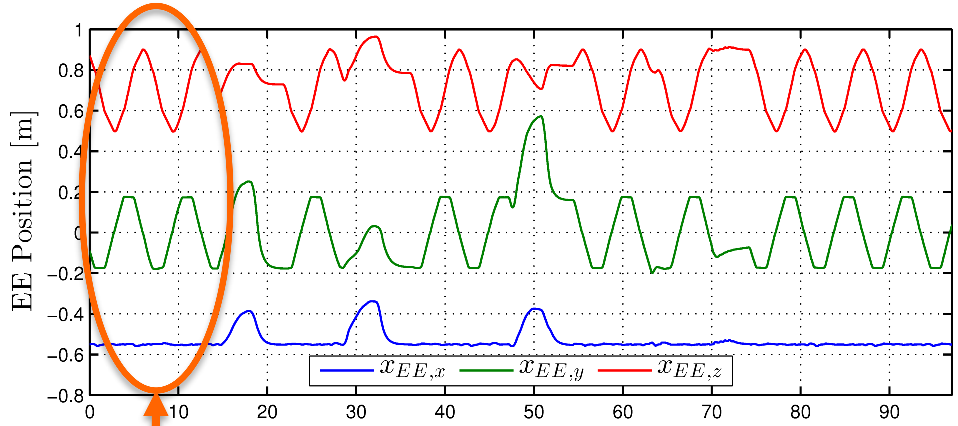

estimated force: $F_{relax} < \|\widehat{\boldsymbol{F}}_c\| \leq F_{abort}$

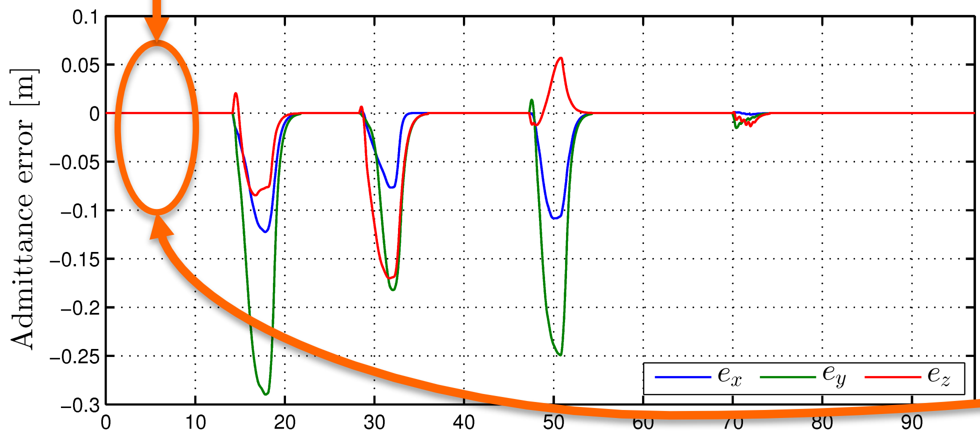

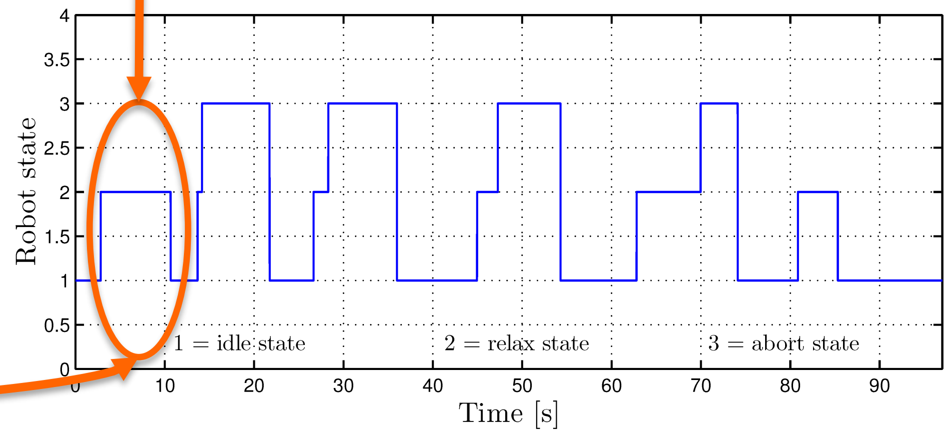

robot in **relax** state, no admittance error...

pHRI experiments

Analysis of results

…and the original task is **abandoned**

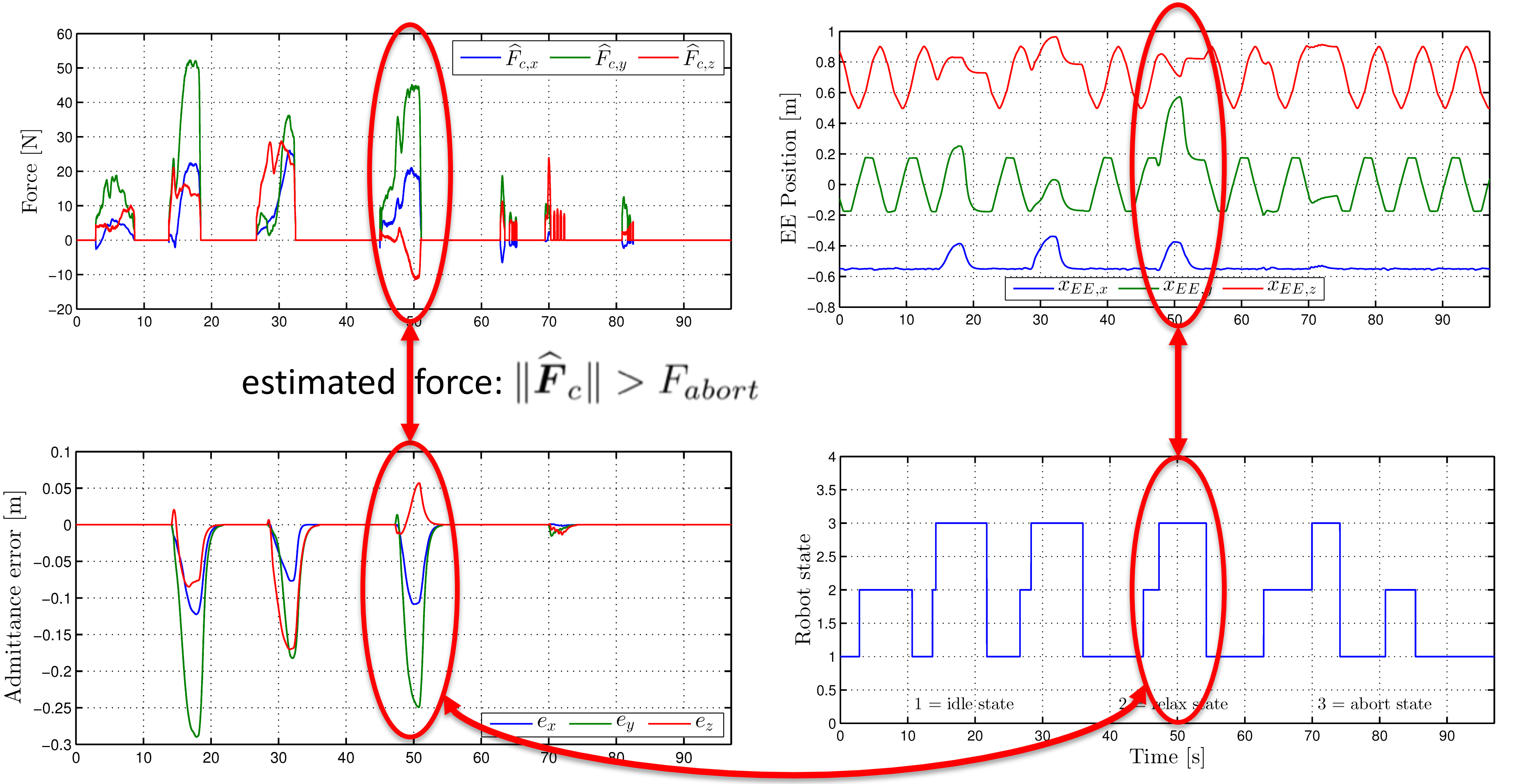

estimated force: $\|\widehat{\boldsymbol{F}}_c\| > F_{abort}$

the robot goes in **abort** state, an admittance error is present…

HRC under a closed control architecture

KUKA KR5 Sixx R650 robot

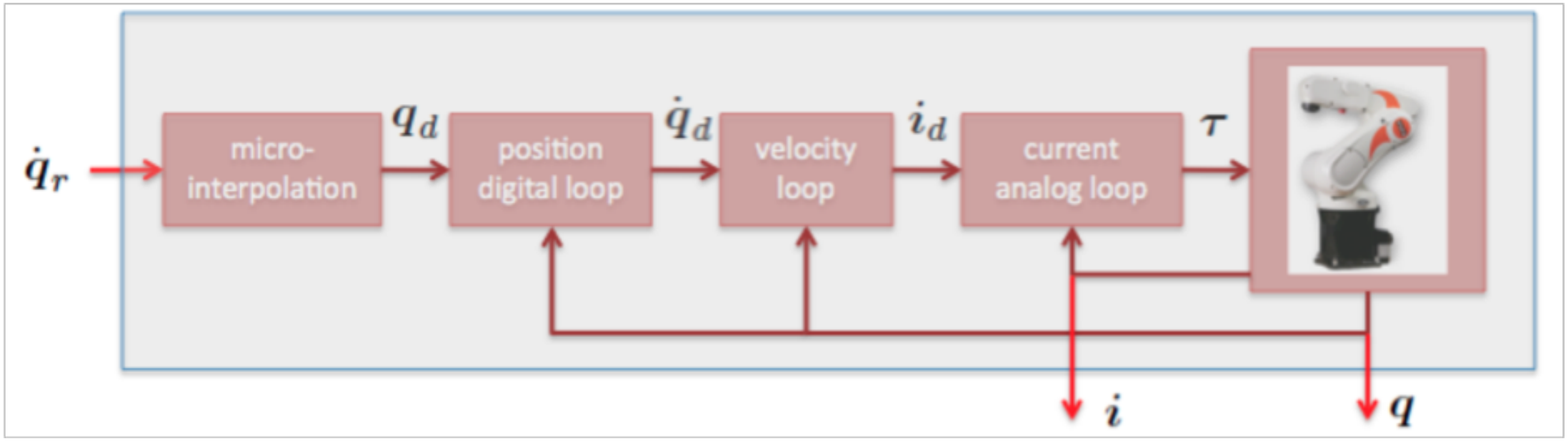

- low-level motor control laws are not known nor accessible by the user
- user programs, based also on other exteroceptive sensors (vision, Kinect, F/T sensor) can be implemented on an external PC via the RSI (RobotSensorInterface), communicating with the KUKA controller every 12 ms
- available robots measures: joint positions (by encoders) and (absolute value of) applied motor currents
- controller reference is given as a velocity or a position in joint space (also Cartesian commands are accepted)

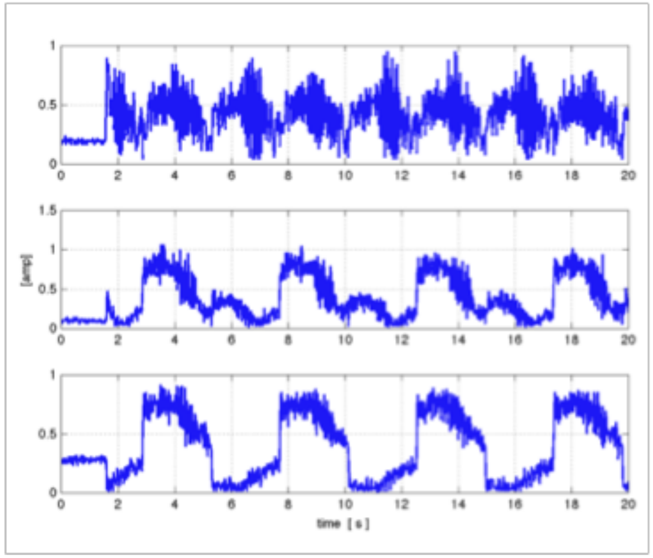

typical motor currents on first three joints

Collision detection and stop

KUKA KR5 Sixx R650 robot (ICRA 2013)

https://youtu.be/18RsAxkf7kk (this and next 3 videos)

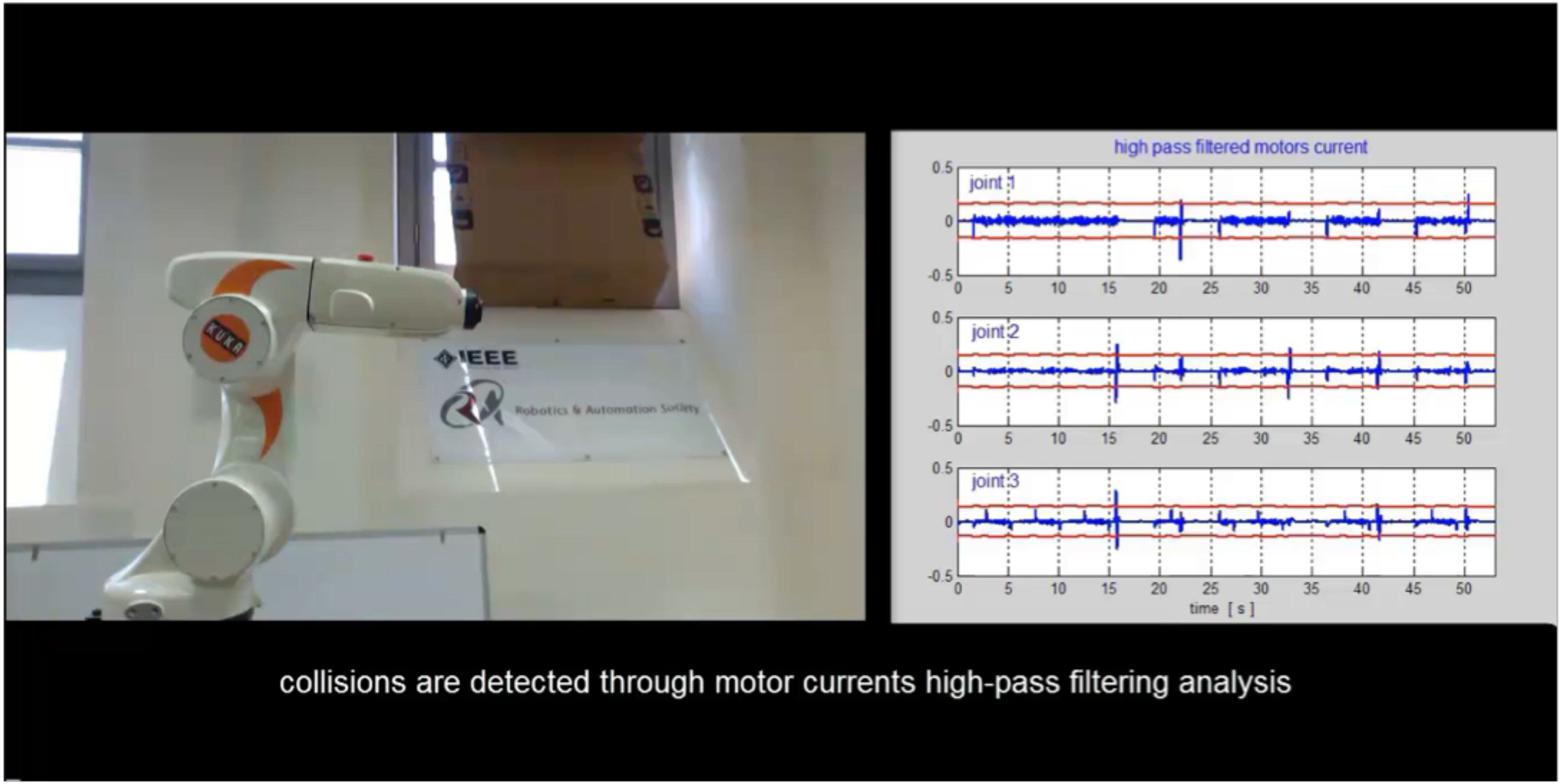

high-pass filtering of motor currents (a signal-based detection...)

Distinguish accidental collisions from intentional contact

… and then collaborate

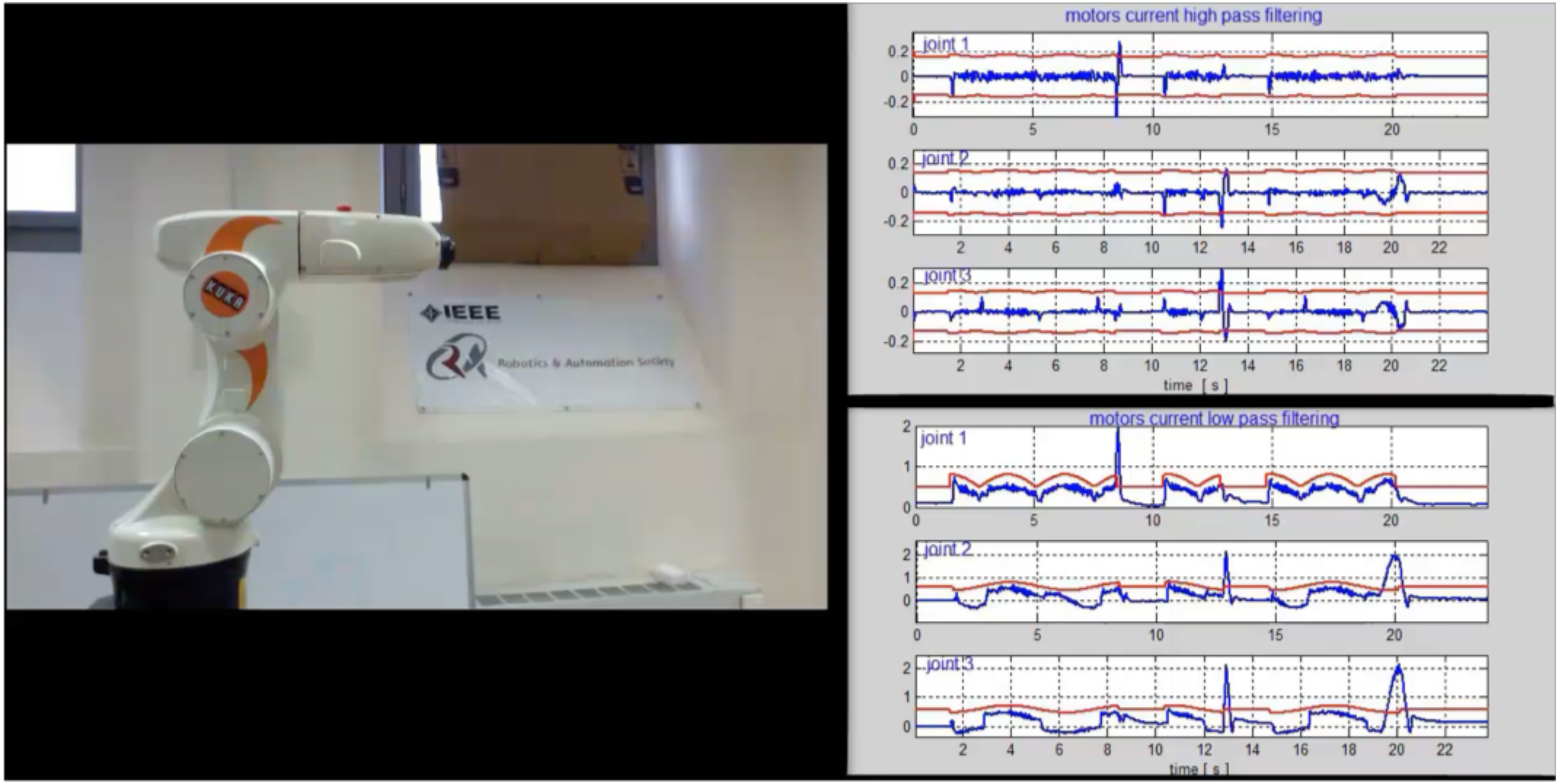

using both high-pass and low-pass filtering of motor currents

— here collaboration mode is manual guidance of the robot

Other possible robot reactions

After collaboration mode has been established

collaboration mode:
pushing/pulling
the robot

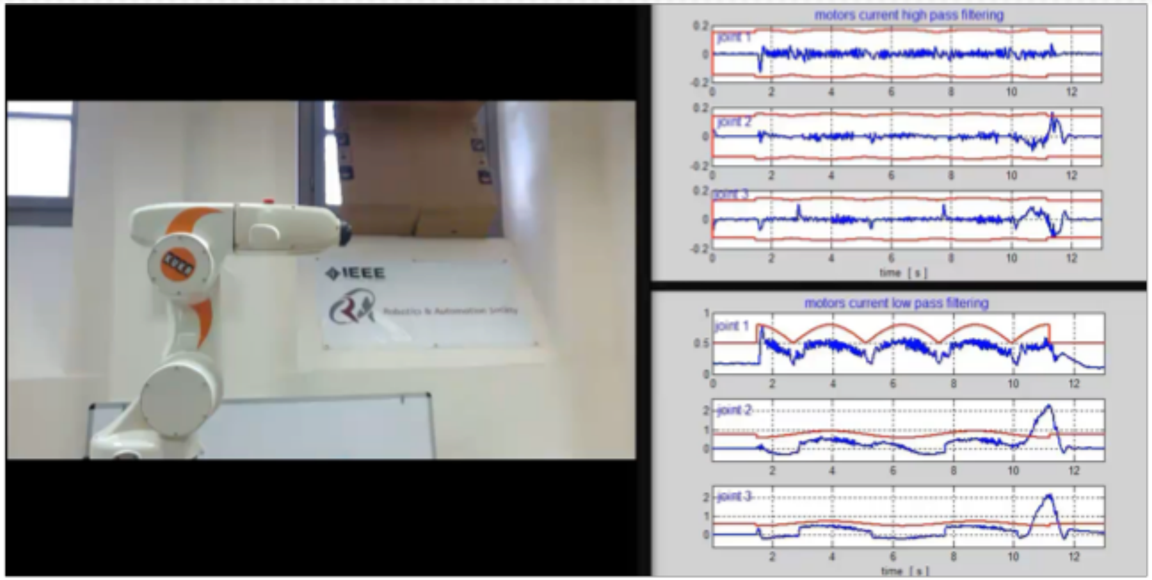

collaboration mode:
compliant-like
robot behavior

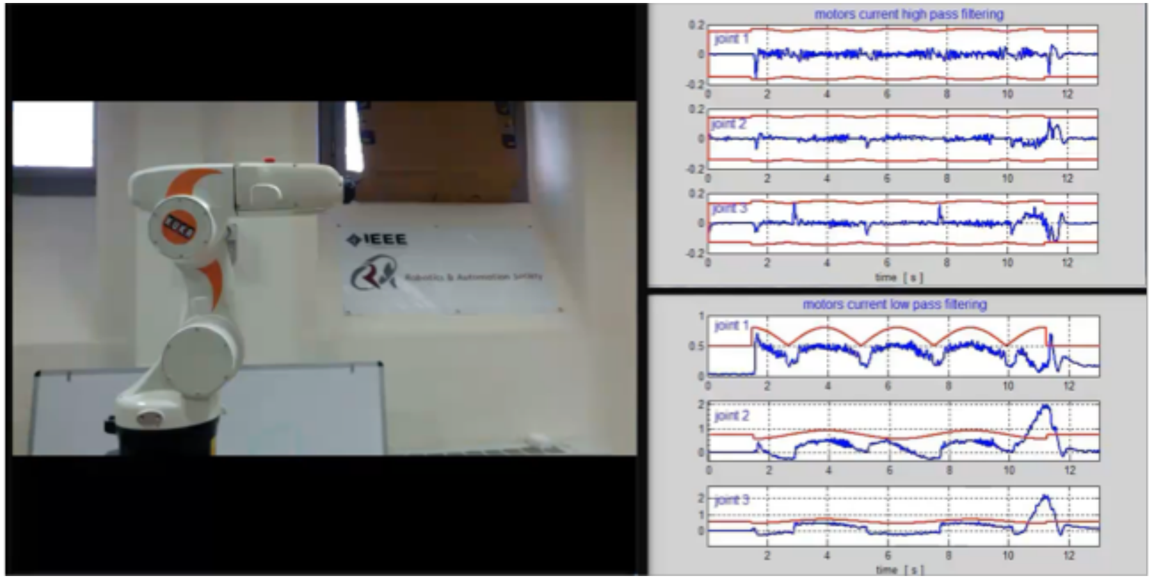

Trials on collision detection and hard/soft contact

With a group of human subjects

26 volunteers (informed students, in the age range 20-24, about 20% female)

a total of **168 collisions**, in series of 5 for each user (with repeated attempts)

collision detection	trial 1	trial 2	trial 3	trial 4	trial 5	total count	% over all trials	% over all attempts	% over last trials
at attempt # 1	19	19	18	23	25	**104**	80%	61.9%	92.6%
at attempt # 2	6	2	4	3	1	**16**	12.3%	9.5%	3.7%
at attempt # 3	1	4	3	0	0	**8**	6.2%	4.8%	0%
at attempt # 4	0	1	1	0	0	**2**	1.5%	1.2%	0%
# of user trials	26	26	26	26	26	**130**	**100%**	-	-
robot fails to stop	8	13	13	3	1	**38**	-	22.6%	3.7%
# of user attempts	34	39	39	29	27	**168**	-	**100%**	**100%**
false stops						**6**	4.6%	3.6%	

416 contacts, **half** of which were intended to be **soft**

distinguishing between soft contacts (S) and accidental collisions (H)	number of soft trials	number of successes	number of fails	% of successes	% of fails
group 1: sequence SSHHSSHH	52	39	13	75.0%	25.0%
group 1: sequence HHSSHHSS	52	44	8	84.6%	15.4%
group 2: sequence SSSSHHHH	52	44	8	84.6%	15.4%
group 2: sequence HHHHSSSS	52	45	7	86.5%	13.5%
overall	**208**	**172**	**36**	**82.7%**	**17.3%**

end-users experience a "learning" process → adapt thresholds!

Conclusions

Toward a safer and efficient control of human-robot physical collaboration

- framework for safe human-robot coexistence and collaboration, based on hierarchy of consistent **controlled** behaviors of the robot
  - residual-based collision detection (and isolation)
  - portfolio of collision reaction algorithms (using also redundancy)
  - real-time collision avoidance based on data processed in depth space
  - distinguishing intentional/soft contacts from accidental/hard collisions
  - estimation of contact force and location, by combining inner/outer sensing
  - admittance/impedance/force/hybrid control laws, generalized at the contact level
  - some useful behavior can be obtained also in poor man situations (closed control architectures, with no access to signals or dynamic information)
  - applications are slowly coming from industrial and service stakeholders

Our team at DIAG

Robotics Lab of the Sapienza University of Rome (back in 2014)

Acknowledgements

@Sapienza – DIAG - **Fabrizio Flacco**†, Claudio Gaz, Milad Geravand, Emanuele Magrini

@DLR – Institute of Robotics and Mechatronics - Alin Albu-Schäffer, Sami Haddadin

@Stanford – Artificial Intelligence Lab - Oussama Khatib, Torsten Kröger

References - 1

Download pdf for personal use at www.diag.uniroma1.it/deluca/Publications

- A. De Luca and R. Mattone, “Sensorless robot collision detection and hybrid force/motion control,” IEEE Int. Conf. on Robotics and Automation, pp. 999-1004, 2005.
- A. De Luca, A. Albu-Schäffer, S. Haddadin, and G. Hirzinger, “Collision detection and safe reaction with the DLR-III lightweight manipulator arm,” IEEE/RSJ Int. Conf. on Intelligent Robots and Systems, pp. 1623-1630, 2006.
- S. Haddadin, A. Albu-Schäffer, A. De Luca, and G. Hirzinger, “Collision detection and reaction: A contribution to safe physical human-robot interaction,” IEEE/RSJ Int. Conf. on Intelligent Robots and Systems, pp. 3356-3363, 2008 (IROS 2008 Best Application Paper Award).
- A. De Luca and L. Ferrajoli, “Exploiting robot redundancy in collision detection and reaction,” IEEE/RSJ Int. Conf. on Intelligent Robots and Systems, pp. 3299-3305, 2008.
- A. De Santis, B. Siciliano, A. De Luca, A. Bicchi, “An atlas of physical human-robot interaction,” Mechanism and Machine Theory, vol. 43, no. 3, pp. 253–270, 2008 (2017 MMT Award for Excellence).
- A. De Luca and L. Ferrajoli, “A modified Newton-Euler method for dynamic computations in robot fault detection and control,” IEEE Int. Conf. on Robotics and Automation, pp. 3359-3364, 2009.
- F. Flacco, A. De Luca, “Multiple depth/presence sensors: Integration and optimal placement for human/robot coexistence,” IEEE Int. Conf. on Robotics and Automation, pp. 3916-3923, 2010.
- F. Flacco, T. Kröger, A. De Luca, and O. Khatib, “A depth space approach to human-robot collision avoidance,” IEEE Int. Conf. on Robotics and Automation, pp. 338-345, 2012.
- A. De Luca and F. Flacco, “Integrated control for pHRI: Collision avoidance, detection, reaction and collaboration,” 4th IEEE RAS/EMBS Int. Conf. on Biomedical Robotics and Biomechatronics, pp. 288-295, 2012 (BioRob 2012 RAS Best Paper Award).
- M. Geravand, F. Flacco, and A. De Luca, “Human-robot physical interaction and collaboration using an industrial robot with a closed control architecture,” IEEE Int. Conf. on Robotics and Automation, pp. 3985-3992, 2013.
- E. Magrini, F. Flacco, and A. De Luca, “Estimation of contact force using a virtual force sensor,” IEEE/RSJ Int. Conf. on Intelligent Robots and System, pp. 2126-2133, 2014.

References - 2

Download pdf for personal use at www.diag.uniroma1.it/deluca/Publications

- F. Flacco, T. Kröger, A. De Luca, and O. Khatib, "A depth space approach for evaluating distance to objects —with application to human-robot collision avoidance," J. of Intelligent & Robotic Systems, vol. 80, suppl. 1, pp. 7-22, 2015.
- E. Magrini, F. Flacco, and A. De Luca, "Control of generalized contact motion and force in physical human-robot interaction," IEEE Int. Conf. on Robotics and Automation, pp. 2298-2304, 2015 (ICRA 2015 Best Conference Paper Award Finalist).
- E. Magrini and A. De Luca, "Hybrid force/velocity control for physical human-robot collaboration tasks," IEEE/RSJ Int. Conf. on Intelligent Robots and Systems. pp. 857-863, 2016.
- F. Flacco and A. De Luca, "Real-time computation of distance to dynamic obstacles with multiple depth sensors," IEEE Robotics and Automation Lett., vol. 2, no. 1, pp. 56-63, 2017.
- E. Magrini, A. De Luca, "Human-robot coexistence and contact handling with redundant robots," IEEE/RSJ Int. Conf. on Intelligent Robots and Systems, pp. 4611-4617, 2017.
- S. Haddadin, A. De Luca, and A. Albu-Schäffer, "Robot collisions: A survey on detection, isolation, and identification," IEEE Trans. on Robotics, vol. 33, no. 6, pp. 1292-1312, 2017.
- C. Gaz, A. De Luca, "Payload estimation based on identified coefficients of robot dynamics --with an application to collision detection, " IEEE/RSJ Int. Conf. on Intelligent Robots and Systems, pp. 3033-3040, 2017.
- C. Gaz, E. Magrini, A. De Luca " A model-based residual approach for human-robot collaboration during manual polishing operations," Mechatronics, vol. 55, pp. 234-247, 2018.
- E. Mariotti, E. Magrini, A. De Luca, "Admittance control for human-robot interaction using an industrial robot equipped with a F/T sensor," IEEE Int. Conf. on Robotics and Automation (submitted), 2019.

- **Videos**: YouTube channel RoboticsLabSapienza. Playlist: Physical human-robot interaction